Volume 4 (2004)
Number 1

COMPUTATIONAL methods in applied MATHEMATICS

OFFPRINT

AN INTERNATIONAL JOURNAL

COMPUTATIONAL METHODS IN APPLIED MATHEMATICS, Vol. 4 (2004), No. 1, pp. 66–93

METHODS FOR NUMERICAL MODELING OF TWO-DIMENSIONAL CAPILLARY SURFACES[1]

VIKTOR K. POLEVIKOV

Belarusian State University, Department of Computational Mathematics
4 F. Skaryna Ave., 220050 Minsk, Belarus

Abstract — Certain methods for numerical solving plane and axially symmetric problems on equilibrium shapes of a capillary surface are presented. The methods possess a high order of approximation on a nonuniform grid. They are easy to realize, fairly universal and suitable for constructing not only simply connected but also doubly connected and disconnected surfaces, including strongly curved ones. It is shown that the iterative algorithms constructed are absolutely stable at each iteration. The condition for convergence of iterations is obtained within the framework of a linear theory. To describe peak-shaped configurations of a magnetic fluid in a high magnetic field, an algorithm of generation of adaptive grid nodes in accordance with the surface curvature is proposed. The methods have been tested for the well-known problems of capillary hydrostatics on equilibrium shapes of a drop adjacent to the horizontal rotating plate under gravity, and of an isolated magnetic-fluid drop in a high uniform magnetic field. It has been established that they adequately respond to the physical phenomenon of a crisis of equilibrium shapes, i.e., they can be adopted to investigate the stability of equilibrium states of a capillary surface.

2000 Mathematics Subject Classification: 65L12; 65D07; 65Z05; 76D45; 76M20.

Keywords: capillary surface, parametric differential equations, numerical modeling, finite-difference method, tangential method, spline-method, computational stability, convergence of iterations, adaptive grid, test problems, computational experiment.

1. Introduction

Just as the majority of practically important problems with a free boundary, the problems on equilibrium shapes of a capillary surface, as a rule, have a complex nonlinear statement. In the general case, we deal with a hydrodynamic problem whose unknown solution is sought in the domain with a preliminarily unknown boundary determined by the unknown solution. Exhaustive reviews of the theoretical methods for investigating equilibrium capillary surfaces are presented in [9, 10]. These reviews show that no methods for numerical modeling of doubly-connected, disconnected as well as simply-connected strongly curved surfaces have been developed in modern computational hydrodynamics.

In [2, 3, 11, 12, 14, 15], the iteration-difference approach was developed. In [10], it is presented as "rather universal because it is suitable for constructing equally both axially symmetric simply- and doubly-connected equilibrium surfaces and cylindrical ones (plane problem)". Also, it should be added that it is efficient in the case of strongly curved surfaces

[1]Partially supported by DAAD and DFG grants

and is easily extended to the class of disconnected surfaces. It can also serve for investigating of the equilibrium-state instability as it adequately responds to a physical crisis of equilibrium shapes.

The subject of this paper includes both a description of numerical methods which are effective in a wide range of two-dimensional equilibrium states up to peak-shaped configurations, and their justification consisting of a theoretical analysis and testing. The paper is organized as follows. In Section 2, we formulate the parametric second-order differential equations of an equilibrium capillary surface in the cases of plane and axially symmetric problems with regard for the gravitational and magnetic forces. A change of variables, which plays an important part in constructing the iterative algorithms presented in the paper, is introduced. In Section 3, a finite-difference scheme approximating the free surface equations with the second order on a nonuniform grid is described. Iterative algorithms for its realization are proposed. Section 4 presents a tangential method designed to solve modified free-surface differential equations with a new unknown being a tangent inclination angle. The computational stability and convergence of iterations are investigated. A spline-method is proposed and analyzed in Section 5. It is based on the approximation of a free surface by cubic splines exactly satisfying the parametric differential problem in grid nodes. In Section 6, we show how to apply the tangential and spline methods in the irregular case where the contact line of a capillary surface is preassigned. Section 7 proposes an a priori method for constructing an adaptive grid whose density of nodes on the surface varies according to the surface curvature. Finally, Section 8 is devoted to the testing of the above-mentioned methods on the well-known magnetic- and nonmagnetic-fluid statics problems with a simply connected surface.

2. Mathematical model of a capillary surface

2.1. General equations

Consider an equilibrium capillary surface Γ of a viscous incompressible magnetic fluid that contacts a nonmagnetic gas medium and is acted on by gravitational and magnetic forces $\mathbf{f}$. The steady-state motion of such a fluid both inside a volume and on a free surface is governed by the equations [4, 8, 16]

$$\begin{aligned} &\nabla p = -\rho(\mathbf{v}\cdot\nabla)\mathbf{v} + \eta\nabla^2\mathbf{v} + \mathbf{f}, \quad \nabla\cdot\mathbf{v} = 0; \\ &\mathbf{f} = \rho\mathbf{g} + \mu_0 M\nabla H \end{aligned} \tag{1}$$

where p is the fluid pressure, ρ is the density, $\mathbf{v}$ is the velocity vector, $\eta = \text{const}$ is the dynamic viscosity, $\mathbf{g}$ is the acceleration of gravity, μ_0 is the magnetic constant, $M = M(H,T)$ is the fluid magnetization, H is the intensity of the magnetic field , T is the temperature.

Boundary conditions on the free surface are obtained from the general balance equations for normal and shear stresses with regard for the capillary and magnetic pressure jumps. If viscous stresses are neglected in the external (gas) medium, then the balance equation for normal stresses on the surface Γ assumes the form [4, 8, 16]

$$p - p_0 = \sigma K - \frac{\mu_0}{2}\left(M\frac{H_n}{H}\right)^2 + 2\eta\frac{\partial v_n}{\partial n} \tag{2}$$

where $p_0 = \text{const}$ is the external pressure, σ is the surface tension coefficient, K is the sum of principal surface curvatures that takes a positive value if the surface is convex, H_n and v_n are the normal components of the magnetic intensity and velocity vectors.

The density ρ and the surface tension σ of the isothermal fluid are given to be constant. In the nonisothermal case, use is made of Boussinesque's approximation taking into account the dependence $\rho(T)$ only in the right term $\mathbf{f}$. For the problems of thermocapillary convection, $\sigma = \sigma(T)$ is assumed.

2.2. Axially symmetric surface

If Γ is the surface of revolution, then its shape is determined by the equilibrium meridian line. Introduce the cylindrical coordinates R, Z by bringing the OZ axis into coincidence with the symmetry axis and directing it opposite to the gravity vector. Let S be an arc length of an unknown meridian line that ranges from $S = 0$ to $S = \ell$. The meridian shape will be described by the parametric functions $R(S)$, $Z(S)$. Then $\mathbf{n} = (-Z', R')$, $\mathbf{t} = (R', Z')$ are the normal and tangent unit vectors to the equilibrium line in the axial-section plane (prime means differentiation with respect to S). Note that the tangent vector $\mathbf{t}$ is oriented in the direction of increasing S. The surface curvature is defined by the formula $K = \phi(RZ')'/(RR')$, where we choose $\phi = -1$ if, while moving along the meridian line in the direction of increasing S, the fluid remains on the right, and $\phi = 1$ if the fluid remains on the left.

In the isothermal case, by means of simple manipulations with Eqs (1) with regard to the equilibrium condition $v_n = \mathbf{v} \cdot \mathbf{n} = 0$, we have on the surface Γ

$$\frac{\partial p}{\partial S} = \nabla p \cdot \mathbf{t} = -\frac{\rho}{2}\frac{\partial (v_S^2)}{\partial S} + \rho \frac{R'}{R} v_\varphi^2 - \eta \frac{1}{R}\frac{\partial (Rw)}{\partial n} - \rho g Z' + \mu_0 \frac{\partial}{\partial S}\int\limits_0^H M dH$$

where v_S and v_φ are the tangential and azimuthal velocity components, and

$$w = \frac{\partial v_Z}{\partial R} - \frac{\partial v_R}{\partial Z}$$

is the vorticity. Hence, for any points $R(S)$, $Z(S)$ of the free surface we find

$$\begin{aligned} &p = \Pi + \text{const}, \\ &\Pi = -\frac{\rho}{2} v_S^2 + \int\limits_0^S \left(\rho \frac{R'}{R} v_\varphi^2 - \eta \frac{1}{R}\frac{\partial (Rw)}{\partial n} - \rho g Z' \right) dS + \mu_0 \int\limits_0^H M dH. \end{aligned} \tag{3}$$

By eliminating the pressure p from Eqs (2) and (3), we obtain a parametric differential equation for the axially symmetric surface Γ

$$\begin{aligned} &Z'' = R'F, \quad 0 < S < \ell; \\ &F = \frac{\phi}{\sigma}\Psi + \text{const} - \frac{Z'}{R}, \quad \Psi = \Pi + \frac{\mu_0}{2}\left(M \frac{H_n}{H} \right)^2 - 2\eta \frac{\partial v_n}{\partial n}. \end{aligned} \tag{4}$$

The natural condition $R'^2 + Z'^2 = 1$ serves as one more equation. By using differentiation, it can be replaced by $R'' = -Z'F$. For the natural condition in this case not to be violated, it should be satisfied, at least, at one value of S, e.g., at $S = 0$ or $S = \ell$.

2.3. Cylindrical surface (plane problem)

In the case of the plane problem, the cylindrical equilibrium surface is determined by the equilibrium line of the cross-section. Introduce into the cross-section plane the Cartesian coordinates X, Y by directing the OY axis opposite to the vector $\mathbf{g}$. In these coordinates $K = \phi Y''/X' = -\phi X''/Y'$, where $X = X(S)$ and $Y = Y(S)$ are the unknown parametric functions describing the shape of the equilibrium line. By analogy with the axially symmetric case, we arrive at the equations

$$Y'' = X'F, \quad X'' = -Y'F, \quad 0 < S < \ell;$$

$$F = \frac{\phi}{\sigma}\Psi + \text{const}, \quad \Psi = \Pi + \frac{\mu_0}{2}\left(M\frac{H_n}{H}\right)^2 - 2\eta\frac{\partial v_n}{\partial n},$$

$$\Pi = -\frac{\rho}{2}v_S^2 + \int_0^S \left(-\eta\frac{\partial w}{\partial n} - \rho g Y'\right) dS + \mu_0 \int_0^H M dH, \quad w = \frac{\partial v_Y}{\partial X} - \frac{\partial v_X}{\partial Y}$$

whose solution requires the condition $X'^2 + Y'^2 = 1$ to be satisfied.

The obtained differential equations are supplemented with the boundary conditions as well as with the non-local (integral) condition of fluid volume conservation. By boundary conditions can be understood either conditions where the fluid contacts a solid wall specified by the wall geometry and a given wetting angle, or symmetry conditions.

2.4. Test problems

To test the algorithms, two hydrostatics problems on axially-symmetric equilibrium shapes of a simply-connected capillary surface were chosen. These are: 1) the problem on a drop adjacent to a horizontal rotating plate under gravity, 2) the problem on an isolated magnetic-fluid drop in a high uniform magnetic field. The first of them is the classical problem of capillary hydrostatics [7,9,10], and the second one is the well-known problem of magnetic-fluid statics [4,8].

2.4.1. Problem 1. Place the origin of coordinates on the plate surface, namely in the middle of the drop base, and let the arc length take the value $S = 0$ at the drop apex (i.e., at $R = 0$) and $S = \ell$ at the point where the meridian contacts the plane $Z = 0$. Since the magnetic forces are absent from Eq. (4), we have $\Psi = \Pi = -\rho g[Z - Z(0)] + 0.5\rho\omega^2 R^2$, where ω is the angular rotational velocity of the drop. So, the equations for the drop surface are obtained as

$$\begin{aligned} &R'' = -Z'F, \quad Z'' = R'F, \quad 0 < S < \ell; \\ &F = \phi\left(-\frac{\rho g}{\sigma}Z + \frac{\rho\omega^2}{2\sigma}R^2\right) - \frac{Z'}{R} + \text{const}. \end{aligned} \tag{5}$$

The boundary conditions follow from the symmetry ones at $S = 0$ and from the conditions where fluid contacts a solid wall at $S = \ell$

$$\begin{aligned} &R(0) = 0, \quad R'(0) = 1, \qquad Z'(0) = 0, \\ &Z(\ell) = 0, \quad R'(\ell) = \cos\alpha, \quad Z'(\ell) = \phi\sin\alpha \end{aligned} \tag{6}$$

where α is the wetting (contact) angle. Assuming that the drop volume V is prescribed, it can be determined as the volume of the body of revolution

$$V = -2\pi\phi \int_0^\ell ZRR'dS. \tag{7}$$

Thus, the mathematical statement of the problem for $R(S)$ and $Z(S)$ consists of the differential Eqs. (5), the boundary conditions (6), and the integral condition (7). The adopted direction of increasing S owes us to choose $\phi = -1$ if the drop is adjacent to the plate from above (sessile drop) and $\phi = 1$ if it is adjacent to the plate from below (pendent drop).

2.4.2. Problem 2. Consider a magnetic-fluid drop not contacting a solid wall and acted on by a high uniform magnetic field under zero-gravity in the state of magnetic saturation. Assume that the vector of the field intensity is collinear to the OZ symmetry axis. Then $\mathbf{f} = \mu_0 M_\infty \nabla H = 0$, $H_n = \pm HR'$ and it should obviously be assumed in Eq. (4) that $\Psi = 0.5\mu_0 M_\infty^2 (R')^2$, where M_∞ is the fluid saturation magnetization. Considering that the drop is symmetric about the equatorial plane $Z = 0$, we restrict ourselves to the half-space $Z \geqslant 0$. As in Problem 1, choose the point $S = 0$ on the OZ axis and the point $S = \ell$ on the plane $Z = 0$. The choice is consistent with $\phi = -1$. Hence, the drop shape is described by the equations

$$\begin{aligned} &R'' = -Z'F, \quad Z'' = R'F, \quad 0 < S < \ell; \\ &F = -\frac{\mu_0 M_\infty^2}{2\sigma}(R')^2 - \frac{Z'}{R} + \text{const}. \end{aligned} \tag{8}$$

The boundary conditions are formulated with regard to the drop symmetry

$$R(0) = Z'(0) = Z(\ell) = R'(\ell) = 0, \quad R'(0) = 1, \quad Z'(\ell) = -1. \tag{9}$$

The mathematical model is closed by an expression that relates the solution to the drop volume V

$$V = 4\pi \int_0^\ell ZRR'dS. \tag{10}$$

2.5. Change of variables

The specific feature of the parametric statement is that the length, ℓ, of the equilibrium line, i.e., the domain of definition of the problem is beforehand unknown. This causes great difficulties for the numerical solution. The procedure of nondimensionalizing is an important element for constructing algorithms of the iteration-difference approach.

Choose ℓ as a characteristic size and introduce dimensionless variables as

$$\bar{s} = \frac{S}{\ell}, \quad \bar{r} = \frac{R}{\ell}, \quad \bar{z} = \frac{Z}{\ell}. \tag{11}$$

It allows us to move the unknown length into the equations and make computations on the fixed interval $[0, 1]$.

2.5.1. *Problem 1.* In the new variables, problem (5) – (7) takes the form

$$\begin{cases} \bar{r}'' = -\bar{z}'(f+C), \quad \bar{z}'' = \bar{r}'(f+C), \quad 0 < \bar{s} < 1, \\ f = \phi(-\mathrm{Bo}L^2\bar{z} + \mathrm{P}L^3\bar{r}^2) - \dfrac{\bar{z}'}{\bar{r}}, \end{cases} \tag{12}$$

$$\begin{cases} \bar{r}(0) = 0, \quad \bar{r}'(0) = 1, & \bar{z}'(0) = 0, \\ \bar{z}(1) = 0, \quad \bar{r}'(1) = \cos(\phi\alpha), & \bar{z}'(1) = \sin(\phi\alpha), \end{cases} \tag{13}$$

$$L = \left(-2\pi\phi \int_0^1 \bar{z}\bar{r}\bar{r}' d\bar{s} \right)^{-1/3}, \tag{14}$$

where $\mathrm{Bo} = \rho g V^{2/3}/\sigma$ is the Bond number that characterizes the gravitational-to-capillary force ratio, $\mathrm{P} = \rho\omega^2 V/(2\sigma)$ is the parameter having the meaning of the centrifugal-to-capillary force ratio, $L = \ell/V^{1/3}$, C is the constant not yet defined.

To define the constant C, write down one of Eqs. (12) as

$$(\bar{r}\,\bar{z}')' = \bar{r}\,\bar{r}'\left[\phi(-\mathrm{Bo}L^2\bar{z} + \mathrm{P}L^3\bar{r}^2) + C\right].$$

Then, having integrated it on the interval $[0, 1]$ with regard to conditions (13) and (14), we obtain

$$C = \phi\left(\frac{2\sin\alpha}{\bar{r}(1)} - \frac{1}{2}\mathrm{P}L^3\bar{r}^2(1)\right) - \frac{\mathrm{Bo}}{\pi L\bar{r}^2(1)}. \tag{15}$$

2.5.2. *Problem 2.* Now formulate problem (8) – 10 in the new variables:

$$\begin{cases} \bar{r}'' = -\bar{z}'(f+C), \quad \bar{z}'' = \bar{r}'(f+C), \quad 0 < \bar{s} < 1, \\ f = -\mathrm{W}L(\bar{r}')^2 - \dfrac{\bar{z}'}{\bar{r}}, \end{cases} \tag{16}$$

$$\bar{r}(0) = \bar{z}'(0) = \bar{z}(1) = \bar{r}'(1) = 0, \quad \bar{r}'(0) = 1, \quad \bar{z}'(1) = -1; \tag{17}$$

$$L = \left(4\pi \int_0^1 \bar{z}\bar{r}\bar{r}' d\bar{s}\right)^{-1/3} = \left(-2\pi \int_0^1 \bar{z}'\bar{r}^2 d\bar{s}\right)^{-1/3}, \tag{18}$$

where $\mathrm{W} = \mu_0 M_\infty^2 V^{1/3}/(2\sigma)$ is the dimensionless parameter that characterizes the ratio of the magnetic pressure jump on a free surface to the capillary jump, $L = \ell/V^{1/3}$.

The dependence of the constant C on the solution is defined as in Problem 1:

$$C = \frac{2}{\bar{r}^2(1)}\left(-\bar{r}(1) + \mathrm{W}L\int_0^1 \bar{r}(\bar{r}')^3 d\bar{s}\right). \tag{19}$$

It should be noted that the main objective to use the change of variables (11) is that we want to obtain an explicit stable formula for correction of the dimensionless length L in iterations while solving the nonlinear free-surface equilibrium problem. This is achieved by the integral condition, which in Problems 1 and 2 reduces to (14) and (18), respectively, and is convenient for recalculating the length L at each iteration of the algorithm of successive refinement of an unknown boundary.

In the algorithm of the iteration-difference method we seek the solution $\bar{r}(\bar{s})$, $\bar{z}(\bar{s})$ that corresponds to the unit length of the equilibrium free-surface line but not the prescribed fluid volume, as the initial statement of the problem requires. Usually the variables $r = R/V^{1/3}$, $z = Z/V^{1/3}$ nondimensionalized by the volume V are used to analyze the result obtained. A transition from variables (11) to them is made by simple recalculation: $r = \bar{r}L$, $z = \bar{z}L$.

3. Finite-difference method

Let us formulate a two-dimensional problem on the equilibrium shape of a capillary surface in the following general form:

$$x'' + y'F = 0, \quad y'' - x'F = 0, \quad 0 < s < 1; \tag{20}$$

$$\begin{cases} x(0) = a, & y(1) = b, \\ x'(0) = \cos\alpha_0, & y'(0) = \sin\alpha_0, \quad x'(1) = \cos\alpha_1, \quad y'(1) = \sin\alpha_1 \end{cases} \tag{21}$$

where $x(s)$ and $y(s)$ are the unknown parametric functions; $F = f + C$; $f = f(x, y, x', y', L)$ is the assigned function; C and L are constants that are functionals of the known form of the solution; a, α_0, b, α_1 are the predetermined constants. Expressions for f and C can also contain functions of a solution whose analytical form is unknown, but their numerical values are determined by solving some additional problem, e.g., a problem on the magnetic field distribution or a hydrodynamic process in the magnetic-fluid volume. In the case of the plane problem x and y that appear here are the dimensionless Cartesian coordinates of the surface, and in the case of the axially symmetric problem by them are understood the cylindrical coordinates r, z.

The identity $x'^2 + y'^2 = 1$ is the natural property of the parametric functions $x(s)$, $y(s)$. From the system (20) it can easily be obtained that if this equality is obeyed at some one value of s, then it is also valid for all $s \in [0, 1]$. In virtue of this, when problem (20), (21) is solved, any of the last four conditions of (21) can be neglected. In addition, one of the remaining three conditions was formally needed to define the dependence of the constant C on the solution (see Subsection 2.5).

Introduce in the interval $[0, 1]$ a nonuniform grid

$$\hat{\omega}_h = \{s_i = s_{i-1} + h_i \mid i = 1, 2, \ldots, N; \ s_0 = 0, \ s_N = 1\}$$

and further denote by x_i, y_i the difference analogs to the exact solution $x(s_i)$, $y(s_i)$ in the grid nodes.

For problem (20), (21) let us construct the difference scheme

$$\Lambda_1(x, y, F)|_i \equiv x_{ss,i} + y_{\hat{s},i}F_i = 0, \quad \Lambda_2(x, y, F)|_i \equiv y_{ss,i} - x_{\hat{s},i}F_i = 0, \ i = 1, 2, \ldots, N-1;$$

$$x_0 = a, \quad x_{s,N-0.5} = \cos\alpha_1 + \frac{h_N}{2}F_N \sin\alpha_1; \tag{22}$$

$$y_{s,0.5} = \sin\alpha_0 + \frac{h_1}{2}F_0\cos\alpha_0, \quad y_N = b$$

where

$$x_{ss,i} = \frac{1}{\hbar_i}\left(x_{s,i+0.5} - x_{s,i-0.5}\right), \quad x_{\hat{s},i} = \left(\frac{1}{2} - \frac{\triangle_i}{12\hbar_i}\right)x_{s,i-0.5} + \left(\frac{1}{2} + \frac{\triangle_i}{12\hbar_i}\right)x_{s,i+0.5};$$

$$F_i = f_i + C, \quad f_i = f(x_i^*, y_i^*, x_{\hat{s},i}, y_{\hat{s},i}, L), \quad i = 1, 2, \ldots, N-1;$$

$$f_0 = f(a, y_0, \cos\alpha_0, \sin\alpha_0, L), \quad f_N = f(x_N, b, \cos\alpha_1, \sin\alpha_1, L);$$

$$x_{s,i-0.5} = \frac{1}{h_i}(x_i - x_{i-1}), \quad x_i^* = \frac{1}{3}(x_{i-1} + x_i + x_{i+1});$$

$$\hbar_i = \frac{1}{2}(h_i + h_{i+1}), \quad \triangle_i = h_{i+1} - h_i.$$

For any sufficiently smooth function $x(s)$ the asymptotic expansions

$$x(s_{i+\gamma}) = x(s_i^*) + \sum_{k=1}^{3} \frac{c_{i+\gamma}^k}{k!} x^{(k)}(s_i^*) + O(\hbar_i^4), \quad \gamma = 0, \pm 1; \quad c_i = -\frac{\triangle_i}{3}, \quad c_{i\pm1} = \pm\hbar_i + \frac{\triangle_i}{6};$$

$$\frac{x(s_i) - x(s_{i-1})}{h_i} = x'(s_i^*) - \frac{c_{i+1}}{2} x''(s_i^*) + \frac{1}{6}\left(\hbar_i^2 + \frac{\triangle_i^2}{12}\right) x'''(s_i^*) + O(\hbar_i^3),$$

$$\frac{x(s_{i+1}) - x(s_i)}{h_{i+1}} = x'(s_i^*) - \frac{c_{i-1}}{2} x''(s_i^*) + \frac{1}{6}\left(\hbar_i^2 + \frac{\triangle_i^2}{12}\right) x'''(s_i^*) + O(\hbar_i^3),$$

$$\frac{1}{3}[x(s_{i-1}) + x(s_i) + x(s_{i+1})] = x(s_i^*) + O(\hbar_i^2)$$

are valid at the point

$$s_i^* = \frac{1}{3}(s_{i-1} + s_i + s_{i+1}) = s_i + \frac{\triangle_i}{3}$$

which can be interpreted as the center of mass of the grid pattern.

As a result of applying these expansions to the functions $x(s)$, $y(s)$, it is obtained that the difference scheme (22) provides the second order of local approximation on an arbitrary nonuniform grid $\hat{\omega}_h$.

To solve the nonlinear difference problem (22), consider two two-layer iterative schemes

$$\begin{cases} \dfrac{1}{\tau}(x_{ss,i}^{n+1} - x_{ss,i}^n) + \Lambda_1(x^n, y^n, F^n)|_i = 0, \quad i = 1, 2, \ldots, N-1, \\ x_0^{n+1} = a, \quad x_{s,N-0.5}^{n+1} = \cos\alpha_1 + \dfrac{h_N}{2} F_N^n \sin\alpha_1, \end{cases} \tag{23}$$

$$\begin{cases} \dfrac{1}{\tau}(y_{ss,i}^{n+1} - y_{ss,i}^n) + \Lambda_2(x^n, y^n, F^n)|_i = 0, \quad i = 1, 2, \ldots, N-1, \\ y_{s,0.5}^{n+1} = \sin\alpha_0 + \dfrac{h_1}{2} F_0^n \cos\alpha_0, \quad y_N^{n+1} = b \end{cases} \tag{24}$$

and

$$\begin{cases} \dfrac{1}{\tau}(x_i^{n+1} - x_i^n) = x_{ss,i}^{n+1} + y_{\hat{s},i}^n F_i^n, \quad i = 1, 2, \ldots, N-1, \\ x_0^{n+1} = a, \quad x_{s,N-0.5}^{n+1} = \cos\alpha_1 + \dfrac{h_N}{2} F_N^n \sin\alpha_1, \end{cases} \tag{25}$$

$$\begin{cases} \dfrac{1}{\tau}(y_i^{n+1} - y_i^n) = y_{ss,i}^{n+1} - x_{\hat{s},i}^n F_i^n, \quad i = 1, 2, \ldots, N-1, \\ y_{s,0.5}^{n+1} = \sin\alpha_0 + \dfrac{h_1}{2} F_0^n \cos\alpha_0, \quad y_N^{n+1} = b, \end{cases} \tag{26}$$

where $n = 0, 1, 2, \ldots$ is the iteration number; $\tau > 0$ is the relaxation parameter; $F_i^n = f_i^n + C^n$.

In the two schemes, the decomposition of the difference operators on iterative layers is carried out so that the upper layer contains only the linear part of the difference equation, namely the second difference derivative with respect to either the coordinate x or the coordinate y of the free surface. Both scheme (23), (24) and scheme (25), (26) are implemented at each iteration by means of the three-point elimination method (Thomas algorithm) applied to problems (23)–(26) which are linear tridiagonal systems. As a result, new iterative approximations x^{n+1} and y^{n+1} are determined, then f^{n+1}, C^{n+1}, $F^{n+1} = f^{n+1} + C^{n+1}$ are calculated. The Thomas algorithm for each of problems (23)–(26) is absolutely stable.

Scheme (23), (24) was successfully used to compute equilibrium shapes of simply-connected [3, 6, 12] and doubly-connected [2, 5, 18, 19] surfaces both in the presence of gravitational, centrifugal and magnetic forces and in their absence under zero-gravity. By means of this scheme, the problem of capillary hydrostatics with an essentially disconnected free surface was solved for the first time [13]. Scheme (25), (26) was adopted to investigate the equilibrium states of a drop rotating in a gravitational field [11].

4. Tangential method

4.1. Description of the algorithm

Introduce into our consideration a new unknown $\beta(s)$ being an angle between the tangent to the equilibrium line $x(s)$, $y(s)$ and the Ox axis. Bearing in mind that $x' = \cos\beta$, $y' = \sin\beta$, problem (20), (21) can be reformulated as

$$\begin{aligned} &\beta' = F, \qquad \beta(0) = \alpha_0, \quad \beta(1) = \alpha_1; \\ &x' = \cos\beta, \quad x(0) = a; \qquad y' = \sin\beta, \quad y(1) = b. \end{aligned} \tag{27}$$

In such a statement, the identity $x'^2 + y'^2 = 1$ is satisfied irrespective of the boundary conditions. Assuming that the conditions $\beta(0) = \alpha_0$ and $\beta(1) = \alpha_1$ have been already used to describe the constant C, it is enough to leave only one of them in problem (27).

On the grid $\hat{\omega}_h$ for problem (27) we consider a difference scheme of the fourth-order approximation

$$\begin{aligned} &\frac{\beta_i - \beta_{i-1}}{h_i} = \Phi_i, && \Phi_i = \frac{F_{i-1} + F_i}{2} - \frac{h_i}{12}(f_i' - f_{i-1}'), \\ &\frac{x_i - x_{i-1}}{h_i} = \mathrm{X}(\beta, F)|_i, && \mathrm{X}(\beta, F)|_i = \frac{u_{i-1} + u_i}{2} + \frac{h_i}{12}(F_i v_i - F_{i-1} v_{i-1}), \\ &\frac{y_i - y_{i-1}}{h_i} = \mathrm{Y}(\beta, F)|_i, && \mathrm{Y}(\beta, F)|_i = \frac{v_{i-1} + v_i}{2} - \frac{h_i}{12}(F_i u_i - F_{i-1} u_{i-1}), \\ &i = 1, 2, \ldots, N; && \beta_0 = \alpha_0, \quad \beta_N = \alpha_1, \quad x_0 = a, \quad y_N = b \end{aligned} \tag{28}$$

where

$$\begin{aligned} &F = f + C, \quad f = f(x, y, u, v, L), \\ &f' = \frac{\partial f}{\partial x} u + \frac{\partial f}{\partial y} v - \frac{\partial f}{\partial u} F v + \frac{\partial f}{\partial v} F u, \quad u = \cos\beta, \quad v = \sin\beta. \end{aligned}$$

If in the expressions for Φ_i, X_i, Y_i the h_i-containing terms are omitted, then the obtained system will be of the second-order approximation with respect to problem (27).

In view of (28), the iterative algorithm for computating free surface coordinates will be constructed as

$$\begin{cases} \beta_i^{n+1} = \beta_{i+1}^{n+1} - h_{i+1}\Phi_{i+1}^n + (1-\tau)(\beta_i^n - \beta_{i+1}^n + h_{i+1}\Phi_{i+1}^n), \\ i = N-1, N-2, \ldots, 1; \quad \beta_N^{n+1} = \alpha_1, \quad \beta_0^{n+1} = \alpha_0, \end{cases} \tag{29}$$

$$x_i^{n+1} = x_{i-1}^{n+1} + h_i \mathrm{X}(\beta^{n+1}, F^n)|_i, \quad i = 1, 2, \ldots, N; \quad x_0^{n+1} = a, \tag{30}$$

$$\begin{cases} y_i^{n+1} = y_{i+1}^{n+1} - h_{i+1}\mathrm{Y}(\beta^{n+1}, F^n)|_{i+1}, \quad i = N-1, N-2, \ldots, 0, \\ y_N^{n+1} = b. \end{cases} \tag{31}$$

Instead of (29), it is possible to use the following procedure:

$$\begin{aligned} &\beta_i^{n+1} = \beta_{i-1}^{n+1} + h_i\Phi_i^n + (1-\tau)(\beta_i^n - \beta_{i-1}^n - h_i\Phi_i^n), \quad i = 1, 2, \ldots, N-1; \\ &\beta_0^{n+1} = \alpha_0, \quad \beta_N^{n+1} = \alpha_1. \end{aligned} \tag{32}$$

Computations at each iteration are conducted by recurrence formulas. First, the recurrence rules (29) or (32) are used to compute the grid values of β_i^{n+1}. Then, by employing procedures (30) and (31), new iterative approximations are determined for the free surface coordinates. And, finally, the grid functions F_i^{n+1} and Φ_i^{n+1} are formed by the found values of x_i^{n+1}, y_i^{n+1}, β_i^{n+1}. The direction of the passage through the nodes in algorithms (30) and (31) obeys the particular statement of the differential problem on a capillary surface shape. For other statements it can be otherwise, not changing the essence of the method.

Bearing in mind the constructive features of the method presented, we shall name it the tangential or the T-method. The obvious advantages of the T-method are: a high order of approximation on a nonuniform grid, an exact approximation of the boundary conditions, a simple design of the algorithm. Unlike the iteration-difference schemes (23), (24) and (25), (26), the T-method provides the difference analog of the condition $x'^2 + y'^2 = 1$ to be satisfied at all nodes, at each iteration and at any τ. In so doing, a better agreement between the iterative solution and the exact solution of the differential problem is attained.

The following second-order approximation scheme is an important modification of the T-method:

$$\begin{aligned} &\frac{\beta_{i+0.5} - \beta_{i-0.5}}{h_i} = \Phi_i, \quad \Phi_i = f\left(x_i + \frac{\triangle_i}{4}u_i, y_i + \frac{\triangle_i}{4}v_i, u_i, v_i, L\right) + C, \; i = 1, 2, \ldots, N-1; \\ &\beta_0 = \alpha_0, \quad \beta_N = \alpha_1; \\ &\frac{\beta_{0.5} - \beta_0}{0.5h_1} = F_0 + \frac{h_1}{4}f_0', \quad \frac{\beta_N - \beta_{N-0.5}}{0.5h_N} = F_N - \frac{h_N}{4}f_N'; \\ &\frac{x_i - x_{i-1}}{h_i} = \cos\beta_{i-0.5}, \quad \frac{y_i - y_{i-1}}{h_i} = \sin\beta_{i-0.5}, \quad i = 1, 2, \ldots, N; \\ &x_0 = a, \quad y_N = b \end{aligned} \tag{33}$$

where

$$u_i = \cos\frac{\beta_{i-0.5} + \beta_{i+0.5}}{2}, \quad v_i = \sin\frac{\beta_{i-0.5} + \beta_{i+0.5}}{2}.$$

The characteristic feature of the scheme (33) is that the grid function β is defined not on the main grid, but on the auxiliary one consisting of the midpoints $s_{i+0.5} = 0.5(s_i + s_{i+1}) = s_i + 0.5h_i$. The definition of the variables on different grids allows to hope for improvement of the main characteristics of the method.

According to (29) – (31), we construct the iterative algorithm for solving the difference problem (33) as

$$\begin{aligned}
&\beta_{i-0.5}^{n+1} = \beta_{i+0.5}^{n+1} - \hbar_i \Phi_i^n + (1-\tau)\left(\beta_{i-0.5}^n - \beta_{i+0.5}^n + \hbar_i \Phi_i^n\right), \ i = N-1, N-2, ..., 2;\\
&\beta_{0.5}^{n+1} = \alpha_0 + \frac{h_1}{2} F_0^n + \frac{h_1^2}{8} f_0'^n, \quad \beta_{N-0.5}^{n+1} = \alpha_1 - \frac{h_N}{2} F_N^n + \frac{h_N^2}{8} f_N'^n;\\
&x_i^{n+1} = x_{i-1}^{n+1} + h_i \cos\beta_{i-0.5}^{n+1}, \quad i = 1, 2, \ldots, N; \qquad x_0^{n+1} = a;\\
&y_i^{n+1} = y_{i+1}^{n+1} - h_{i+1} \sin\beta_{i+0.5}^{n+1}, \quad i = N-1, N-2, \ldots, 0; \quad y_N^{n+1} = b.
\end{aligned} \tag{34}$$

As we can see in Subsection 6.1, scheme (34) can be applied not only to problems with a moving boundary, i.e., with given wetting angles as in (27), but to problems with given contact points as well.

4.2. Computational stability

Assume that a computational error appears at the $(n+1)$-th iteration in the boundary conditions so that the conditions $\tilde\beta_N^{n+1} = \alpha_1 + \delta_N$, $\tilde x_0^{n+1} = a + \xi_0$, $\tilde y_N^{n+1} = b + \eta_N$ are in fact utilized in algorithms (29) – (31). When affected by small errors δ_N, ξ_0 and η_N at the $(n+1)$-th iteration, we obtain the following solution $\tilde\beta_i^{n+1} = \beta_i^{n+1} + \delta_i$, $\tilde x_i^{n+1} = x_i^{n+1} + \xi_i$, $\tilde y_i^{n+1} = y_i^{n+1} + \eta_i$, $i = 0, 1, \ldots, N$. Considering that the grid functions β^{n+1}, x^{n+1}, y^{n+1} also obey Eqs (29) – (31), a computational error at grid nodes is described by the relations

$$\delta_i = \delta_{i+1} = \delta_{i+2} = \ldots = \delta_N; \tag{35}$$

$$\begin{aligned}
\xi_i &= \xi_{i-1} + h_i\Big\{\frac{1}{2}\left[\left(\cos\tilde\beta_{i-1}^{n+1} - \cos\beta_{i-1}^{n+1}\right) + \left(\cos\tilde\beta_i^{n+1} - \cos\beta_i^{n+1}\right)\right]\\
&\quad + \frac{1}{12} h_i\left[F_i^n\left(\sin\tilde\beta_i^{n+1} - \sin\beta_i^{n+1}\right) - F_{i-1}^n\left(\sin\tilde\beta_{i-1}^{n+1} - \sin\beta_{i-1}^{n+1}\right)\right]\Big\}\\
&= \xi_0 - \sum_{k=1}^{i}\Big\{h_k\left[\sin\frac{\delta_{k-1}}{2}\sin\left(\beta_{k-1}^{n+1} + \frac{\delta_{k-1}}{2}\right) + \sin\frac{\delta_k}{2}\sin\left(\beta_k^{n+1} + \frac{\delta_k}{2}\right)\right]\\
&\quad + \frac{h_k^2}{6}\left[F_{k-1}^n \sin\frac{\delta_{k-1}}{2}\cos\left(\beta_{k-1}^{n+1} + \frac{\delta_{k-1}}{2}\right) - F_k^n \sin\frac{\delta_k}{2}\cos\left(\beta_k^{n+1} + \frac{\delta_k}{2}\right)\right]\Big\};
\end{aligned} \tag{36}$$

$$\begin{aligned}
\eta_{i-1} &= \eta_i - h_i\Big\{\frac{1}{2}\left[\left(\sin\tilde\beta_{i-1}^{n+1} - \sin\beta_{i-1}^{n+1}\right) + \left(\sin\tilde\beta_i^{n+1} - \sin\beta_i^{n+1}\right)\right]\\
&\quad - \frac{1}{12} h_i\left[F_i^n\left(\cos\tilde\beta_i^{n+1} - \cos\beta_i^{n+1}\right) - F_{i-1}^n\left(\cos\tilde\beta_{i-1}^{n+1} - \cos\beta_{i-1}^{n+1}\right)\right]\Big\}\\
&= \eta_N - \sum_{k=i}^{N}\Big\{h_k\left[\sin\frac{\delta_{k-1}}{2}\cos\left(\beta_{k-1}^{n+1} + \frac{\delta_{k-1}}{2}\right) + \sin\frac{\delta_k}{2}\cos\left(\beta_k^{n+1} + \frac{\delta_k}{2}\right)\right]\\
&\quad + \frac{h_k^2}{6}\left[F_{k-1}^n \sin\frac{\delta_{k-1}}{2}\sin\left(\beta_{k-1}^{n+1} + \frac{\delta_{k-1}}{2}\right) - F_k^n \sin\frac{\delta_k}{2}\sin\left(\beta_k^{n+1} + \frac{\delta_k}{2}\right)\right]\Big\}
\end{aligned} \tag{37}$$

where $i = 1, 2, \ldots, N$.

Equalities (35) point to the absolute stability of procedure (29) in the sense of boundary conditions. Based on relations (36) and (37) with regard to (35), it is easy to make the

following rough estimates:

$$|\xi_i| \leqslant |\xi_0| + |\delta_N| \left(1 + \frac{1}{6} \max_{1 \leqslant k \leqslant N} (h_k |F_k^n|)\right),$$
$$|\eta_i| \leqslant |\eta_N| + |\delta_N| \left(1 + \frac{1}{6} \max_{1 \leqslant k \leqslant N} (h_k |F_k^n|)\right), \quad i = 0, 1, \ldots, N.$$

They mean that procedures (30) and (31) are also stable. Hence the algorithm for the realization of the tangential method at each iteration is absolutely stable. The influence of the function F on the computational errors ξ_i and η_i is not dangerous because the value of $|\delta_N|$ is close to zero and, as a rule, the product $F_k h_k$ is small at the grid nodes. What is more, the estimates are improved on the uniform grid of spacing h

$$|\xi_i| \leqslant |\xi_0| + |\delta_N| \left(1 + \frac{h^2}{6} \max_{1 \leqslant k \leqslant N} |F_k^n|\right), \quad |\eta_i| \leqslant |\eta_N| + |\delta_N| \left(1 + \frac{h^2}{6} \max_{1 \leqslant k \leqslant N} |F_k^n|\right).$$

4.3. Convergence of iterations

The convergence of the iterative process (29) – (31) as $n \to \infty$ can be investigated, assuming that the function F does not depend on a solution, i.e., $\Phi_i^n = \Phi_i$ at all $n = 0, 1, 2, \ldots$ In this case, iterations are made only according to algorithm (29). Let β_i be an unknown difference solution. Designate the iterative error as $\varepsilon_i^n = \beta_i^n - \beta_i$, $i = 0, 1, \ldots, N$, $n = 0, 1, 2, \ldots$ where ε^0 is the initial iterative approximation. Assuming $\varepsilon_0^n = \varepsilon_N^n = 0$ and substituting $\beta^n = \beta + \varepsilon^n$ into (29) yield for the error the problem

$$\varepsilon_i^{n+1} - (1 - \tau)\varepsilon_i^n = \varepsilon_{i+1}^{n+1} - (1 - \tau)\varepsilon_{i+1}^n, \quad i = N - 1, N - 2, \ldots, 1; \quad \varepsilon_N^{n+1} = 0$$

which is decomposed into a system of equalities

$$\varepsilon_i^{n+1} - (1 - \tau)\varepsilon_i^n = 0, \quad i = 1, 2, \ldots, N - 1.$$

Hence the error at the n-th iteration is related to the error of the initial approximation by

$$\varepsilon_i^n = (1 - \tau)\varepsilon_i^{n-1} = (1 - \tau)^2 \varepsilon_i^{n-2} = \ldots = (1 - \tau)^n \varepsilon_i^0, \quad i = 0, 1, \ldots, N.$$

From this it follows that the condition

$$0 < \tau < \tau^* = 2 \tag{38}$$

is necessary and sufficient for convergence of the iterations as $n \to \infty$.

Condition (38) results from the linear approximation. Experience shows (see Subsection 8.2) that as the nonlinearity grows, the convergence domain $(0, \tau^*)$ gradually narrows, tending to zero ($\tau^* \to 0$).

It is similarly possible to prove that the iterative scheme (34) also is absolutely stable in the sense of boundary conditions, and its convergence in the linear case is ensured by condition (38).

5. Spline-method

Consider the problem on equilibrium capillary-surface shapes in formulation (20), (21), using for brevity its matrix representation

$$\begin{gathered}\mathbf{x}'' = F\mathbf{I}\mathbf{x}', \quad \mathbf{x} = \begin{bmatrix} x_1(s) \\ x_2(s) \end{bmatrix}, \quad \mathbf{I} = \begin{bmatrix} 0 & -1 \\ 1 & 0 \end{bmatrix}, \quad 0 < s < 1; \\ x_1(0) = a, \quad x_2(1) = b, \quad \mathbf{x}'(0) = \begin{bmatrix} \cos\alpha_0 \\ \sin\alpha_0 \end{bmatrix}, \quad \mathbf{x}'(1) = \begin{bmatrix} \cos\alpha_1 \\ \sin\alpha_1 \end{bmatrix}\end{gathered} \tag{39}$$

where $x_1(s)$, $x_2(s)$ are the unknown parametric functions, $F = f + C$, $f = f(\mathbf{x}, \mathbf{x}', L)$.

5.1. Description of the algorithm

The construction of the spline-method (S-method) is based on the approximation of the functions $x_1(s)$ and $x_2(s)$ by cubic splines satisfying the differential problem (39) on the grid $\hat{\omega}_h$. So, let

$$\begin{aligned}\mathbf{x}(s) \approx \mathbf{P}(s) = \Bigg\{ & \mathbf{m}_{i-1}\frac{(s_i - s)^3}{6h_i} + \mathbf{m}_i\frac{(s - s_{i-1})^3}{6h_i} + \left(\mathbf{x}_{i-1} - \frac{h_i^2}{6}\mathbf{m}_{i-1}\right)\frac{s_i - s}{h_i} \\ & + \left(\mathbf{x}_i - \frac{h_i^2}{6}\mathbf{m}_i\right)\frac{s - s_{i-1}}{h_i} \;\Bigg|\; s \in [s_{i-1}, s_i],\ i = 1, 2, \ldots, N \Bigg\}\end{aligned} \tag{40}$$

where

$$\mathbf{P}(s) = \begin{bmatrix} P_1(s) \\ P_2(s) \end{bmatrix}, \quad \mathbf{x}_i = \begin{bmatrix} x_{1;i} \\ x_{2;i} \end{bmatrix} = \mathbf{x}(s_i), \quad \mathbf{m}_i = \begin{bmatrix} m_{1;i} \\ m_{2;i} \end{bmatrix} = \mathbf{P}''(s_i).$$

At inner nodes, the unknown vectors $\mathbf{x}_i$ and $\mathbf{m}_i$ are connected by the smoothness condition of spline (40)

$$\begin{gathered}\mathbf{P}'(s_i) = \mathbf{x}_{s,i-0.5} - \frac{h_i^2}{6}\mathbf{m}_{s,i-0.5} + \frac{h_i}{2}\mathbf{m}_i = \mathbf{x}_{s,i+0.5} - \frac{h_{i+1}^2}{6}\mathbf{m}_{s,i+0.5} - \frac{h_{i+1}}{2}\mathbf{m}_i, \\ i = 1, 2, \ldots, N-1.\end{gathered} \tag{41}$$

In the following, we use the notation

$$\begin{gathered}\mathbf{q}_i = \mathbf{x}_{s,i-0.5} - \frac{h_i^2}{6}\mathbf{m}_{s,i-0.5} = \mathbf{P}'(s_i) - \frac{h_i}{2}\mathbf{m}_i = \mathbf{P}'(s_{i-1}) + \frac{h_i}{2}\mathbf{m}_{i-1}, \quad i = \overline{1, N}; \\ \mathbf{q}_0 = \mathbf{P}'(0) - \frac{h_0}{2}\mathbf{m}_0 = \mathbf{q}_1 - h_1\mathbf{m}_0, \quad \mathbf{q}_N = \mathbf{P}'(1) - \frac{h_N}{2}\mathbf{m}_N, \quad h_0 = h_1.\end{gathered}$$

With this notation,

$$\begin{gathered}\mathbf{m}_i = \frac{h_{i+1}}{\hbar_i}\mathbf{q}_{s,i+0.5}, \quad \mathbf{P}'(s_i) = \mathbf{q}_i + \frac{h_i}{2}\mathbf{m}_i = \frac{1}{2\hbar_i}\left(h_{i+1}\mathbf{q}_i + h_i\mathbf{q}_{i+1}\right), \quad i = \overline{0, N-1}; \\ \mathbf{x}_{s,i-0.5} = \mathbf{q}_i + \frac{h_i}{6}\left(\frac{h_{i+1}}{\hbar_i}\mathbf{q}_{s,i+0.5} - \frac{h_i}{\hbar_{i-1}}\mathbf{q}_{s,i-0.5}\right), \quad i = \overline{1, N-1}.\end{gathered}$$

According to the idea of the method, let us require that the spline $\mathbf{P}(s)$ satisfies exactly the boundary-value problem (39) on the grid $\hat{\omega}_h$

$$\mathbf{m}_i = F_i\mathbf{I}\mathbf{P}'(s_i), \quad i = 0, 1, \ldots, N;$$

$$\mathbf{P}'(0) = \mathbf{x}'(0), \quad \mathbf{P}'(1) = \mathbf{x}'(1), \quad P_1(0) = a, \quad P_2(1) = b.$$

From here we obtain the difference problem for $\mathbf{q}_i$ and $\mathbf{x}_i$

$$\begin{cases} \mathbf{q}_{s,i+0.5} = \dfrac{1}{h_{i+1}} \left(\hat{\rho}_i \mathbf{I} \mathbf{q}_i + \rho_i \mathbf{I} \mathbf{q}_{i+1} \right), \quad i = 0, 1, \ldots, N-1 \\ \mathbf{q}_0 = \mathbf{x}'(0) - 0.5 h_0 \mathbf{m}_0, \quad \mathbf{q}_N = \mathbf{x}'(1) - 0.5 h_N \mathbf{m}_N \end{cases} \tag{42}$$

$$\mathbf{x}_{s,i-0.5} = \mathbf{q}_i + \frac{h_i}{6} \left(\mathbf{m}_i - \mathbf{m}_{i-1} \right), \quad i = 1, 2, \ldots, N; \quad x_{1;0} = a, \quad x_{2;N} = b \tag{43}$$

where

$$\rho_i = \frac{1}{2} h_i F_i, \quad \hat{\rho}_i = \frac{1}{2} h_{i+1} F_i;$$

$$\mathbf{m}_i = \frac{h_{i+1}}{\hbar_i} \mathbf{q}_{s,i+0.5}, \quad i = \overline{1, N-1}; \quad \mathbf{m}_0 = F_0 \mathbf{I} \mathbf{x}'(0), \quad \mathbf{m}_N = F_N \mathbf{I} \mathbf{x}'(1).$$

At given values of F_0, F_1,..., F_N, problem (42), (43) is a system of linear algebraic equations which decomposes into several subsystems with triangular matrices. Moreover, the solution $\mathbf{q}_i = [q_{1;i}, q_{2;i}]^T$ of system (42) does not depend on the solution $\mathbf{x}_i = [x_{1;i}, x_{2;i}]^T$ of system (43) consisting of two independent subsystems with respect to $x_{1;i}$ and $x_{2;i}$. Taking into consideration the peculiar features of the difference problem, the iterative algorithm for calculating the grid vector-functions $\mathbf{q}_i$ and $\mathbf{x}_i$ is organized as

$$\begin{cases} \mathbf{q}_i^{n+1} = \mathbf{B}_i^n \mathbf{q}_{i+1}^{n+1} + (1-\tau) \left(\mathbf{q}_i^n - \mathbf{B}_i^n \mathbf{q}_{i+1}^n \right), \quad i = N-1, N-2, \ldots, 1; \\ \mathbf{q}_0^{n+1} = (\mathbf{E} - \rho_0^n \mathbf{I}) \, \mathbf{x}'(0), \quad \mathbf{q}_N^{n+1} = (\mathbf{E} - \rho_N^n \mathbf{I}) \, \mathbf{x}'(1), \end{cases} \tag{44}$$

$$\begin{cases} x_{1;i}^{n+1} = x_{1;i-1}^{n+1} + h_i q_{1;i}^{n+1} + \dfrac{h_i^2}{6} \left(m_{1;i}^{n+1} - m_{1;i-1}^{n+1} \right), \\ i = 1, 2, \ldots, N; \quad x_{1;0}^{n+1} = a, \end{cases} \tag{45}$$

$$\begin{cases} x_{2;i}^{n+1} = x_{2;i+1}^{n+1} - h_{i+1} q_{2;i+1}^{n+1} - \dfrac{h_{i+1}^2}{6} \left(m_{2;i+1}^{n+1} - m_{2;i}^{n+1} \right), \\ i = N-1, N-2, \ldots, 0; \quad x_{2;N}^{n+1} = b, \end{cases} \tag{46}$$

where $\mathbf{E}$ is the identity matrix;

$$\mathbf{B}_i = \begin{bmatrix} b_i^0 & b_i^1 \\ -b_i^1 & b_i^0 \end{bmatrix}, \quad b_i^0 = \frac{1 - \rho_i \hat{\rho}_i}{1 + \hat{\rho}_i^2}, \quad b_i^1 = \frac{\rho_i + \hat{\rho}_i}{1 + \hat{\rho}_i^2};$$

$$\mathbf{m}_i = \frac{h_{i+1}}{\hbar_i} \mathbf{q}_{s,i+0.5}, \quad i = \overline{1, N-1}; \quad \mathbf{m}_0 = \frac{2}{h_0} \left[\mathbf{x}'(0) - \mathbf{q}_0 \right], \quad \mathbf{m}_N = \frac{2}{h_N} \left[\mathbf{x}'(1) - \mathbf{q}_N \right].$$

Notice that in algorithm (44) the boundary conditions are given on both the right side and the left side. This enables us to go from one node to another not only in the direction from right to left but from left to right as well. In the latter case, the values of $\mathbf{q}_i^{n+1}$ are calculated at inner nodes by the rule

$$\mathbf{q}_i^{n+1} = \left(\mathbf{B}_{i-1}^n \right)^T \mathbf{q}_{i-1}^{n+1} + (1-\tau) \left[\mathbf{q}_i^n - \left(\mathbf{B}_{i-1}^n \right)^T \mathbf{q}_{i-1}^n \right], \quad i = \overline{1, N-1}. \tag{47}$$

The constructed iterative scheme is economical and easy to realize. At the $(n+1)$-th iteration, first the vector recursive procedure (44) (or the alternative procedure (47)) is

fulfilled and, as a result, the couples $q_{1;i}^{n+1}$, $q_{2;i}^{n+1}$ are determined at all $i = 0, 1, \ldots, N$. Then these values are used in the scalar recursive procedures (45) and (46) which are executed independently of one another, and yield new iterative approximations $x_{1;i}^{n+1}$ and $x_{2;i}^{n+1}$ of the free-surface coordinates. With the found vectors $\mathbf{q}_i^{n+1}$ and $\mathbf{x}_i^{n+1}$ the nonlinear grid function F_i^{n+1} is calculated, thus completing the $(n+1)$-th iteration.

5.2. Stability and iterative convergence

It is possible to analyze the stability of the iterative spline-scheme and the convergence of iterations by analogy with those for the tangential method.

First we consider the computational stability of the recursive procedures (44) – (46) in the sense of boundary conditions. Let $\tilde{\alpha}_1 = \alpha_1 + \delta_1$, $\tilde{a} = a + \eta_{1;0}$, $\tilde{b} = b + \eta_{2;N}$ be the perturbed boundary values at the $(n+1)$-th iteration under which problem (44) – (46) has the solution $\tilde{\mathbf{q}}_i^{n+1} = \mathbf{q}_i^{n+1} + \xi_i$, $\tilde{x}_{1;i}^{n+1} = x_{1;i}^{n+1} + \eta_{1;i}$, $\tilde{x}_{2;i}^{n+1} = x_{2;i}^{n+1} + \eta_{2;i}$. The grid functions ξ_i, $\eta_{1;i}$, $\eta_{2;i}$ represent computational errors at the grid nodes at the $(n+1)$-th iteration resulting from the small perturbations δ_1, $\eta_{1;0}$, $\eta_{2;N}$ of the boundary conditions. As problems (44) and (45) are linear with respect to $\mathbf{q}_i^{n+1}$, $x_{1;i}^{n+1}$, the errors ξ_i and $\eta_{1;i}$ obey the equations

$$\xi_i = \mathbf{B}_i^n \xi_{i+1}, \quad i = N-1, N-2, \ldots, 1;$$

$$\xi_N = (\mathbf{E} - \rho_N^n \mathbf{I})\,[\tilde{\mathbf{x}}'(1) - \mathbf{x}'(1)] = \begin{bmatrix} \cos\tilde{\alpha}_1 - \cos\alpha_1 + \rho_N^n\,(\sin\tilde{\alpha}_1 - \sin\alpha_1) \\ \sin\tilde{\alpha}_1 - \sin\alpha_1 - \rho_N^n\,(\cos\tilde{\alpha}_1 - \cos\alpha_1) \end{bmatrix};$$

$$\eta_{1;i} = \eta_{1;i-1} + h_i\xi_{1;i} + \frac{h_i^2}{6}\left(\frac{\xi_{1;i+1} - \xi_{1;i}}{\hbar_i} - \frac{\xi_{1;i} - \xi_{1;i-1}}{\hbar_{i-1}}\right), \quad i = 1, 2, \ldots, N-1;$$

$$\eta_{1;N} = \eta_{1;N-1} + h_N\xi_{1;N} + \frac{h_N^2}{6}\left[\frac{2}{h_N}(\cos\tilde{\alpha}_1 - \cos\alpha_1 - \xi_{1;N}) - \frac{\xi_{1;N} - \xi_{1;N-1}}{\hbar_{N-1}}\right].$$

In view of the linearity of problem (46) with respect to $q_{2;i}^{n+1}$, $x_{2;i}^{n+1}$ similar equations can also be written for the error $\eta_{2;i}$.

Using these relations, we can estimate the computational error ξ_i in the Euclidean norm

$$\|\xi_N\| = \sqrt{\xi_{1;N}^2 + \xi_{2;N}^2} = 2c_1\,|\sin(0.5\delta_1)| \leqslant c_1\,|\delta_1|, \quad c_1 = \sqrt{1 + (\rho_N^n)^2};$$

$$\|\xi_i\| = \|\mathbf{B}_i^n\xi_{i+1}\| = \sqrt{\frac{1+\rho_i^2}{1+\hat{\rho}_i^2}}\,\|\xi_{i+1}\| = \sqrt{\frac{1+\rho_i^2}{1+\hat{\rho}_i^2}\frac{1+\rho_{i+1}^2}{1+\hat{\rho}_{i+1}^2}}\,\|\xi_{i+2}\|$$

$$= \ldots = \sqrt{\prod_{k=i}^{N-1}\frac{1+\rho_k^2}{1+\hat{\rho}_k^2}}\,\|\xi_N\|, \quad i = 1, 2, \ldots, N-1.$$

The inequality $1 + x \leqslant \exp(x)$ applied to the right side of the previous equality gives

$$\sqrt{\prod_{k=i}^{N-1}\frac{1+\rho_k^2}{1+\hat{\rho}_k^2}} \leqslant \sqrt{\prod_{k=i}^{N-1}(1 + |\hat{\rho}_k^2 - \rho_k^2|)} \leqslant \exp\left(\frac{1}{2}\sum_{k=i}^{N-1}|\hat{\rho}_k^2 - \rho_k^2|\right)$$

$$\leqslant c_2 = \exp\left(\frac{1}{4}\max_{1\leqslant k\leqslant N-1}\left(F_k^2\,|\triangle_k|\right)\right).$$

Thus, it has been proved that

$$\max_{0\leqslant i\leqslant N-1} \|\xi_i\| \leqslant c_2 \|\xi_N\| \leqslant c_1 c_2 |\delta_1| .$$

In the case of a uniform grid, we have $c_2 = 1$, i.e. $\|\xi_i\| = \|\xi_N\|$ at all $i = \overline{1, N-1}$.

Based on the foregoing and taking into consideration the step property $h_1+h_2+\ldots+h_N = 1$ it is not difficult to estimate the error $\eta_{1;i}$:

$$\begin{aligned}
|\eta_{1;i}| &\leqslant |\eta_{1;i-1}| + h_i c_2 \|\xi_N\| \leqslant |\eta_{1;i-2}| + (h_{i-1} + h_i) c_2 \|\xi_N\| \\
&\leqslant \ldots \leqslant |\eta_{1;0}| + c_2 \|\xi_N\| , \quad i = 1, 2, \ldots, N-1; \\
|\eta_{1;N}| &\leqslant |\eta_{1;N-1}| + \frac{2}{3} h_N c_2 \|\xi_N\| + \frac{h_N}{3} (\cos\tilde{\alpha}_1 - \cos\alpha_1) \\
&\leqslant |\eta_{1;0}| + c_2 \|\xi_N\| + \frac{2}{3} h_N \left| \sin\frac{\delta_1}{2} \sin\frac{\tilde{\alpha}_1 + \alpha_1}{2} \right| \leqslant |\eta_{1;0}| + c_2 \|\xi_N\| + |\delta_1| .
\end{aligned}$$

The estimate for $\eta_{2;i}$ is deduced analogously and is of the form

$$\max_i |\eta_{2;i}| \leqslant |\eta_{2;N}| + c_2 \|\xi_N\| + |\delta_1| .$$

The estimates obtained show that small perturbations of the boundary conditions at the $(n+1)$-th iteration lead to small errors in the calculation of $\mathbf{q}_i^{n+1}$ and $\mathbf{x}_i^{n+1}$ at any step of the grid. It means that the recursive procedures (44) – (46) are absolutely stable at each iteration.

The convergence of the iterative process (44) – (46) has been investigated in a linear approximation as $n \to \infty$. It is assumed that $F(s)$ does not depend on the solution and is the known function of the arc length s. Under this assumption, iterations are carried out only by algorithm (44). Let $\varepsilon_i^n = \mathbf{q}_i^n - \mathbf{q}_i$ be the iterative error at the node s_i at the n-th iteration where $\mathbf{q}_i$ is the exact solution of the difference problem, $\mathbf{q}_i^0$ is the initial iterative approximation, and ε_i^0 is the error of the initial approximation. If we assume that the boundary data a, b, α_0, α_1 are given exactly and substitute $\mathbf{q}_i^n = \mathbf{q}_i + \varepsilon_i^n$ into the linear Eq. (44), then we obtain the following problem for the iterative error:

$$\varepsilon_i^{n+1} - (1-\tau)\varepsilon_i^n = \mathbf{B}_i \left[\varepsilon_{i+1}^{n+1} - (1-\tau)\varepsilon_{i+1}^n\right] = \ldots = \mathbf{B}_i \mathbf{B}_{i+1} \ldots \mathbf{B}_{N-1} \left[\varepsilon_N^{n+1} - (1-\tau)\varepsilon_N^n\right],$$

$$i = 1, 2, \ldots, N-1; \quad \varepsilon_0^{n+1} = \varepsilon_0^n = 0, \quad \varepsilon_N^{n+1} = \varepsilon_N^n = 0.$$

From here it follows that

$$\varepsilon_i^n = (1-\tau)\varepsilon_i^{n-1} = (1-\tau)^2 \varepsilon_i^{n-2} = \ldots = (1-\tau)^n \varepsilon_i^0,$$

$$i = 1, 2, \ldots, N-1; \quad \varepsilon_0^n = \varepsilon_N^n = 0.$$

Consequently, the condition $0 < \tau < 2$ is necessary and sufficient for the convergence of the iterative spline-scheme at $n \to \infty$. Notice that the same condition of convergence was previously obtained for the tangential method.

6. Surfaces with a given contact line

The methods described in Sections 3 – 5 are adapted for solving problems on equilibrium capillary surface with an unknown contact line. The contact line position on a smooth solid wall is defined by the given wetting angles α_0 and α_1, the fluid volume and external forces. It is customary to call problems of this kind moving boundary problems.

Problems with a given contact line also occupy an important place in the capillary hydrodynamics and its applications. For example, the well-known problem of applied hydromechanics on the purification of materials and growing of monocrystals aboard space stations under zero-gravity [10] fits into this category. For definiteness, we shall name such problems fixed boundary problems. The boundary conditions for them are of the form $x(0) = a_0$, $x(1) = a_1$, $y(0) = b_0$, $y(1) = b_1$. Such conditions can take place if the contact points are not regular on a solid surface, i.e., the solid surface has a fracture at them.

6.1. Tangential method

Consider the formulation of the fixed boundary problem in the variables $x(s)$, $y(s)$, $\beta(s)$

$$\begin{aligned} &\beta' = F, \quad x' = \cos\beta, \quad y' = \sin\beta; \\ &x(0) = a_0, \quad x(1) = a_1, \quad y(0) = b_0, \quad y(1) = b_1. \end{aligned} \tag{48}$$

We approximate the differential problem (48) on the grid $\hat{\omega}_h$ by means of the modified tangential second-order scheme (33)

$$\begin{gathered} \frac{\beta_{i+0.5} - \beta_{i-0.5}}{h_i} = \Phi_i, \quad \Phi_i = f\left(x_i + \frac{\triangle_i}{4}u_i,\, y_i + \frac{\triangle_i}{4}v_i,\, u_i,\, v_i,\, L\right) + C, \\ u_i = \cos\frac{\beta_{i-0.5} + \beta_{i+0.5}}{2}, \quad v_i = \sin\frac{\beta_{i-0.5} + \beta_{i+0.5}}{2}, \quad i = 1, 2, \ldots, N-1; \\ \frac{x_i - x_{i-1}}{h_i} = \cos\beta_{i-0.5}, \quad \frac{y_i - y_{i-1}}{h_i} = \sin\beta_{i-0.5}, \quad i = 1, 2, \ldots, N; \\ x_0 = a_0, \quad x_N = a_1, \quad y_0 = b_0, \quad y_N = b_1. \end{gathered} \tag{49}$$

Notice that the difference scheme (49) not only does not require any additional approximations in comparison with (33), but is saved from the difference equations approximating the differential equation $\beta' = F$ at the points $s = 0$ and $s = 1$.

From the boundary relations $x_1 - a_0 = h_1\cos\beta_{0.5}$ and $y_1 - b_0 = h_1\sin\beta_{0.5}$, it is not difficult to deduce a formula for the calculation of $\beta_{0.5}$

$$\beta_{0.5} = 2\operatorname{arctan}\frac{y_1 - b_0}{h_1 + x_1 - a_0}.$$

From the viewpoint of computational stability, it is better to use this formula at $x_1 - a_0 \geqslant 0$. Otherwise its following modification is preferable

$$\beta_{0.5} = 2\operatorname{arccot}\frac{y_1 - b_0}{h_1 - x_1 + a_0}.$$

Analogous formulas are valid for $\beta_{N-0.5}$.

Using them in scheme (34), we obtain the iterative algorithm for solving the difference problem (49). Let us write it for the case $a_1 - x_{N-1} \geqslant 0$

$$\begin{gathered}
\beta_{i-0.5}^{n+1} = \beta_{i+0.5}^{n+1} - \hbar_i \Phi_i^n + (1-\tau)\left(\beta_{i-0.5}^n - \beta_{i+0.5}^n + \hbar_i \Phi_i^n\right), \\
i = N-1, N-2, \ldots, 1; \quad \beta_{N-0.5}^{n+1} = 2\arctan\frac{b_1 - y_{N-1}^n}{h_N + a_1 - x_{N-1}^n}; \\
x_i^{n+1} = x_{i-1}^{n+1} + h_i \cos\beta_{i-0.5}^{n+1}, \quad i = \overline{1, N-1}; \quad x_0^{n+1} = a_0, \quad x_N^{n+1} = a_1; \\
y_i^{n+1} = y_{i-1}^{n+1} + h_i \sin\beta_{i-0.5}^{n+1}, \quad i = \overline{1, N-1}; \quad y_0^{n+1} = b_0, \quad y_N^{n+1} = b_1.
\end{gathered} \tag{50}$$

The constant C can be calculated in the iterations of algorithm (50) by the formula

$$C = \left(\beta_{N-0.5} - \beta_{0.5} - \int_{0.5h_1}^{1-0.5h_N} f\, ds\right) \Big/ \left(1 - \frac{h_1 + h_N}{2}\right)$$

which is obtained as a result of the integration of the equation $\beta' = F$ on the interval $[s_{0.5}, s_{N-0.5}]$.

The absolute stability of scheme (50) in the sense of boundary conditions is proved as in Subsection 4.2. The nonlinearity of the formulas for calculating $\beta_{0.5}$ and $\beta_{N-0.5}$ hinders the analysis of the convergence of iterations. Apparently, condition (38) is only necessary for the convergence.

6.2. Spline-method

Formulate the fixed boundary problem in the matrix form

$$\begin{gathered}
\mathbf{x}'' = F\mathbf{I}\mathbf{x}', \quad \mathbf{x}(0) = \mathbf{a}, \quad \mathbf{x}(1) = \mathbf{b}; \quad \mathbf{x}' \cdot \mathbf{x}' = 1; \\
\mathbf{x} = \begin{bmatrix} x_1(s) \\ x_2(s) \end{bmatrix}, \quad \mathbf{I} = \begin{bmatrix} 0 & -1 \\ 1 & 0 \end{bmatrix}, \quad \mathbf{a} = \begin{bmatrix} a_1 \\ a_2 \end{bmatrix}, \quad \mathbf{b} = \begin{bmatrix} b_1 \\ b_2 \end{bmatrix}.
\end{gathered} \tag{51}$$

We approximate the solution $\mathbf{x}(s)$ by the cubic spline $\mathbf{P}(s)$ of form (40) which satisfies Eq. (51) at all grid nodes, i.e., it is assumed that the equalities $\mathbf{P}''(s_i) = F_i\mathbf{I}\mathbf{P}'(s_i)$ are realized at all $i = 0, 1, \ldots, N$. Let us write these equalities in detail using the smoothness condition (41)

$$\mathbf{m}_{i-1} = F_{i-1}\mathbf{I}\left(\mathbf{x}_{s,i-0.5} - \frac{h_i}{3}\mathbf{m}_{i-1} - \frac{h_i}{6}\mathbf{m}_i\right), \quad \mathbf{m}_i = F_i\mathbf{I}\left(\mathbf{x}_{s,i-0.5} + \frac{h_i}{6}\mathbf{m}_{i-1} + \frac{h_i}{3}\mathbf{m}_i\right),$$
$$i = 1, 2, \ldots, N.$$

Considering that the pair of these equations at each number i as a linear system with respect to vectors $\mathbf{m}_{i-1}$ and $\mathbf{m}_i$ and solving it, we find

$$\begin{gathered}
\mathbf{m}_{i-1} = \frac{F_{i-1}}{c_i^2 + d_i^2}\mathbf{V}_i\mathbf{I}\mathbf{x}_{s,i-0.5}, \quad \mathbf{m}_{i+1} = \frac{F_{i+1}}{c_{i+1}^2 + d_{i+1}^2}\mathbf{U}_{i+1}\mathbf{I}\mathbf{x}_{s,i+0.5}, \\
\mathbf{m}_i = \frac{F_i}{c_i^2 + d_i^2}\mathbf{U}_i\mathbf{I}\mathbf{x}_{s,i-0.5} = \frac{F_i}{c_{i+1}^2 + d_{i+1}^2}\mathbf{V}_{i+1}\mathbf{I}\mathbf{x}_{s,i+0.5}, \quad i = \overline{1, N-1}
\end{gathered} \tag{52}$$

where $\mathbf{U}_i = u_{1,i}\mathbf{E} + u_{2,i}\mathbf{I}$ and $\mathbf{V}_i = v_{1,i}\mathbf{E} + v_{2,i}\mathbf{I}$ are nonsingular matrices 2×2,

$$c_i = \frac{2}{3}(\rho_i - \hat{\rho}_{i-1}), \quad d_i = 1 + \frac{1}{3}\hat{\rho}_{i-1}\rho_i, \quad \rho_i = \frac{1}{2}h_iF_i, \quad \hat{\rho}_i = \frac{1}{2}h_{i+1}F_i,$$

$$u_{1,i} = d_i - \hat{\rho}_{i-1}c_i, \quad u_{2,i} = c_i + \hat{\rho}_{i-1}d_i, \quad v_{1,i} = d_i + \rho_i c_i, \quad v_{2,i} = c_i - \rho_i d_i.$$

Substitution of expressions (52) into the smoothness condition (41) results in the system

$$\begin{gathered} h_i(c_i^2 + d_i^2)\mathbf{V}_{i+1}(\mathbf{x}_{i+1} - \mathbf{x}_i) - h_{i+1}(c_{i+1}^2 + d_{i+1}^2)\mathbf{U}_i(\mathbf{x}_i - \mathbf{x}_{i-1}) = 0, \\ i = 1, 2, \ldots, N-1; \quad \mathbf{x}_0 = \mathbf{a}, \quad \mathbf{x}_N = \mathbf{b} \end{gathered} \tag{53}$$

in which the unknowns are the vectors $\mathbf{x}_i$, $i = 1, 2, \ldots, N-1$.

It is possible to improve the matrix of system (53) by multiplying the i-th equation of the system by the nonsingular matrix

$$h_{i+1}\left(c_{i+1}^2 + d_{i+1}^2\right)\mathbf{U}_i^T + h_i\left(c_i^2 + d_i^2\right)\mathbf{V}_{i+1}^T$$

at all $i = 1, 2, \ldots, N-1$. As a result, an equivalent system of the form

$$\begin{gathered} (A_i - \varphi_i\mathbf{I})\mathbf{x}_{i-1} - C_i\mathbf{x}_i + (B_i + \varphi_i\mathbf{I})\mathbf{x}_{i+1} = 0, \\ i = 1, 2, \ldots, N-1; \quad \mathbf{x}_0 = \mathbf{a}, \quad \mathbf{x}_N = \mathbf{b} \end{gathered} \tag{54}$$

is obtained, where

$$A_i = \bar{A}_i + \psi_i, \quad \bar{A}_i = \frac{h_{i+1}}{h_i}\left(1 + \hat{\rho}_{i-1}^2\right)\left(c_{i+1}^2 + d_{i+1}^2\right) > 0,$$

$$B_i = \bar{B}_i + \psi_i, \quad \bar{B}_i = \frac{h_i}{h_{i+1}}\left(1 + \rho_{i+1}^2\right)\left(c_i^2 + d_i^2\right) > 0, \quad C_i = A_i + B_i > 0,$$

$$\varphi_i = u_{1,i}v_{2,i+1} - u_{2,i}v_{1,i+1}, \quad \psi_i = u_{1,i}v_{1,i+1} + u_{2,i}v_{2,i+1}.$$

We construct the iterative algorithm for solving problem (54) choosing the values of the coefficients A_i, B_i, φ_i and ψ_i, which depend in a complicated way on the solution, from the previous iteration

$$\begin{gathered} (A_i^n - \varphi_i^n\mathbf{I})\mathbf{x}_{i-1}^{n+1} - C_i^n\mathbf{x}_i^{n+1} + (B_i^n + \varphi_i^n\mathbf{I})\mathbf{x}_{i+1}^{n+1} = 0, \\ i = 1, 2, \ldots, N-1; \quad \mathbf{x}_0^{n+1} = \mathbf{a}, \quad \mathbf{x}_N^{n+1} = \mathbf{b}. \end{gathered} \tag{55}$$

System (55) is linear with respect to the unknowns $\mathbf{x}_i^{n+1}$ at the upper iterative layer and is of canonical form for the block-elimination method [17]. But, in general, the sufficient stability condition of the method is not satisfied in this case. Considering that the matrix of the system is very sparse, the standard Gaussian elimination procedure may be efficient.

From the viewpoint of the organization of computations, the following algorithm is simpler:

$$\begin{gathered} \left(\bar{A}_i^n + (\psi_i^n)^+\right)\mathbf{x}_{i-1}^{n+1} - \left(\bar{A}_i^n + \bar{B}_i^n + 2(\psi_i^n)^+\right)\mathbf{x}_i^{n+1} + \left(\bar{B}_i^n + (\psi_i^n)^+\right)\mathbf{x}_{i+1}^{n+1} \\ = -\varphi_i^n\mathbf{I}\left(\mathbf{x}_{i+1}^n - \mathbf{x}_{i-1}^n\right) - (\psi_i^n)^-\left(\mathbf{x}_{i-1}^n + \mathbf{x}_{i+1}^n - 2\mathbf{x}_i^n\right), \quad i = 1, 2, \ldots, N-1; \\ \mathbf{x}_0^{n+1} = \mathbf{a}, \quad \mathbf{x}_N^{n+1} = \mathbf{b} \end{gathered} \tag{56}$$

where $\psi^{\pm} = 0.5(\psi \pm |\psi|)$. At the upper iterative layer, we have two independent linear tridiagonal systems (for $x_{1;i}^{n+1}$ and $x_{2;i}^{n+1}$ respectively). Each of them is solved by the Thomas algorithm which is absolutely stable here.

To improve the convergence of the iterative algorithms (55) and (56), it is expedient to use a relaxation procedure similar to the iterative schemes described above.

It should be noted that the construction of spline-scheme (54) does not ensure the natural identity $\mathbf{x}' \cdot \mathbf{x}' = 1$. It is possible to eliminate this deficiency by a suitable evaluation of the constant C. Let us integrate the equation $\mathbf{x}' \cdot \mathbf{x}' = 1$ on the interval $[0, 1]$ in view of Eqs (51)

$$\int_0^1 \mathbf{x}' \cdot \mathbf{x}' ds = (\mathbf{x} \cdot \mathbf{x}')|_0^1 - \int_0^1 \mathbf{x} \cdot \mathbf{x}'' ds = \mathbf{b} \cdot \mathbf{x}'(1) - \mathbf{a} \cdot \mathbf{x}'(0) - \int_0^1 \mathbf{x} \cdot (f + C)\mathbf{I}\mathbf{x}' ds = 1.$$

From here we obtain the formula

$$C = \frac{1}{D}\left(\mathbf{b} \cdot \mathbf{P}'(1) - \mathbf{a} \cdot \mathbf{P}'(0) - \int_0^1 f\mathbf{P} \cdot (\mathbf{I}\mathbf{P}')ds - 1\right)$$

where

$$D = \int_0^1 \mathbf{P} \cdot (\mathbf{I}\mathbf{P}')ds = \int_0^1 (-P_1 P_2' + P_2 P_1')ds.$$

In solving concrete problems, it is not difficult to make the coefficient D distinct from zero by appropriately choosing the origin of coordinates.

7. Adaptive grid

Numerical modeling of a free magnetic-fluid surface subjected to a high magnetic field presents a considerable difficulty because of the peak-shaped structures arising on the surface. With strengthening field, curvature at some points of the surface can increase thousands of times. Computing such configurations requires specific approaches based on the application of adaptive grids.

Introduce a new independent variable $t \in [0, 1]$ and assume that it is related to the dimensionless arc length s by the one-to-one transformation $s(t) \in G$, where G is the set of functions $g(t)$ increasing on the interval $[0, 1]$ such that $g(0) = 0$, $g(1) = 1$. Further we denote by dots the derivatives with respect to t. Then problem (20), (21) can be written with respect to $x(t)$, $y(t)$ as

$$\begin{gathered}(\dot{x}/\dot{s})^{\cdot} + \dot{y}(f + C) = 0, \quad (\dot{y}/\dot{s})^{\cdot} - \dot{x}(f + C) = 0, \quad 0 < t < 1; \\ x(0) = a, \quad y(1) = b; \quad \dot{x}(0) = \dot{s}(0)\cos\alpha_0, \quad \dot{y}(0) = \dot{s}(0)\sin\alpha_0, \\ \dot{x}(1) = \dot{s}(1)\cos\alpha_1, \quad \dot{y}(1) = \dot{s}(1)\sin\alpha_1\end{gathered} \tag{57}$$

where $f = f(x, y, \dot{x}/\dot{s}, \dot{y}/\dot{s}, L)$.

For the variable t, let us build a uniform grid $\omega_h = \{t_i = ih \mid i = 0, 1, \ldots, N;\ h = 1/N\}$. The transformation $s(t)$ maps it into the grid $\hat{\omega}_h$ which is nonuniform with respect to the natural variable s. At a fixed partition number N the accuracy of the difference solution of a surface-shape problem strongly depends on the distribution of nodes s_i. We thus arrive at a problem on the optimal choice of nodes to minimize the error of the difference solution.

An adaptive grid can be constructed in a simpler way if one can find the appropriate transformation $s(t)$ only on the basis of preliminary information or intuitive assumptions

on the structure of the solution sought. So, concerning problem (16) – (19), it is known [4, 8] that as W grows, the drop of the magnetic fluid extends along the direction of the magnetic field and forms a peak-shaped vertex. In addition, the surface curvature decreases monotonically as we come down from the peak. Thus, if we assume that the density of the nodes s_i in $[0, 1]$ varies according to the curvature, then the transformation $s(t)$ can be assigned by the formula [1]

$$s(t) = s(t, a) = -a + \frac{2(a+1)}{1 + (1 + 2/a)^{1-t}}; \quad a = \text{const} > 0. \tag{58}$$

The function $s(t)$ of the form of (58) is defined and ranges over the interval $[0, 1]$. It performs the contraction mapping in the direction of the drop vertex $s = 0$ at the expense of the extension of the domain adjacent to the equatorial line $s = 1$. The degree of contraction is controlled by the parameter a. The lesser a, the higher the degree of contraction. Hence transformation (58) maps the uniform grid $\omega_h = \{t_i\}$ into the nonuniform grid $\hat{\omega}_h = \{s_i = s(t_i)\}$ which is denser near the vertex. This corresponds to the expected structure of the difference solution to problem (16) – (19). Since $\dot{s}(t) > 0$ and $\ddot{s}(t)$ is bounded on the interval $[0, 1]$, this grid $\{s_i\}$ belongs to the family of so-called quasi-uniform grids.

The parameter a depends on the drop shape and is determined so that the product of the dimensionless curvature, $k(0) = \mathrm{W}L - C$, at the vertex by the step $h_1 = s_1 - s_0 = s(h, a)$ is constant for any W and is equal to the product of the curvature, $k_0 = \pi$, of the spherical drop at $\mathrm{W} = 0$ by the step h of the uniform grid. This condition results in the equation for a

$$(\mathrm{W}L - C)\left(-a + \frac{2(a+1)}{1 + (1 + 2/a)^{1-h}}\right) = \pi h. \tag{59}$$

In using transformation (58) and (59), problem (16) – (19), which is of the form of (57), can be approximated on the grid ω_h by the difference second-order scheme

$$\frac{1}{h}\left(\frac{r_{t,i+0.5}}{\dot{s}_{i+0.5}} - \frac{r_{t,i-0.5}}{\dot{s}_{i-0.5}}\right) + \frac{1}{2}\left(z_{t,i-0.5} + z_{t,i+0.5}\right)\left(f_i + C\right) = 0,$$

$$\frac{1}{h}\left(\frac{z_{t,i+0.5}}{\dot{s}_{i+0.5}} - \frac{z_{t,i-0.5}}{\dot{s}_{i-0.5}}\right) - \frac{1}{2}\left(r_{t,i-0.5} + r_{t,i+0.5}\right)\left(f_i + C\right) = 0,$$

$$f_i = -\mathrm{W}L\left(\frac{r_{t,i-0.5} + r_{t,i+0.5}}{2\dot{s}_i}\right)^2 - \frac{z_{t,i-0.5} + z_{t,i+0.5}}{2r_i\dot{s}_i}, \quad i = 1, 2, \ldots, N-1;$$

$$r_0 = 0, \quad r_N = r_{N-1} - \frac{h^2}{2}\dot{s}_N^2\left(\frac{1}{r_N} + C\right);$$

$$z_0 = z_1 + \frac{h^2}{4}\dot{s}_0^2\left(\mathrm{W}L - C\right), \quad z_N = 0$$

where for convenience bars over variables are omitted. The integrals in expressions for L and C are approximated by a quadrature formula of second-order accuracy. For the scheme realization it is possible to use iterative algorithms of the type of (23), (24) or (25), (26). As the magnetic parameter W increases, Eq. (59) can be solved at each its value by the Newton method with L and C corresponding to the previous value of W.

8. Tests

8.1. Organization of computational experiment

The iterative schemes were tested on problems (12) – (15) and (16) – (19). It is known that the existence of equilibrium states in Problem 1 is limited by the small values of the rotation parameter $\mathrm{P} < \mathrm{P}_c(\alpha, \mathrm{Bo})$ and in the case of a pendent drop ($\phi = 1$) also of the Bond number $\mathrm{Bo} < \mathrm{Bo}_c(\alpha, \mathrm{P})$, at whose excess an equilibrium crisis occurs. The choice of Problem 1 as a test one is explained by our wish to compare the critical values of Bo_c and P_c obtained by a sign of computational instability of the iterative schemes with the known data of the linear theory for stability of equilibrium capillary surfaces. It was assumed that a value of the Bond number or the rotation parameter exceeded the critical one if at this value iterations diverged. The critical values of Bo_c and P_c were refined by the dichotomy method unless their error became less than $\delta = 5 \cdot 10^{-4}$.

As for Problem 2, the mechanism of physical collapse of equilibrium shapes was revealed neither theoretically nor experimentally [4, 8]. As the parameter W grows, the magnetic-fluid drop is elongated along the field direction, without breaking. In this case, the surface curvature K increases at the drop apexes and decreases near the equatorial line. Problem 2 is a good tool to test iterative schemes for "strength", since the onset of instability when schemes are implemented, may be only computational in nature. It has been found [12] that as the parameter W grows, the apex curvature $K(0)$ increases almost according to the linear law so that the influence of the parameter W on the convergence of iterations can be interpreted as the influence of the curvature.

Hereinafter in this section, for brevity, the iteration-difference schemes (23), (24) and (25), (26) are referred to as schemes A and B, respectively, the tangential fourth-order approximation method (29) – (31) as scheme *T-4*, its simplified version of the second-order approximation (see Subsection 4.1) as scheme *T-2*, the modified tangential method (34) as scheme *TM-2*, and the iterative spline-scheme (44) – (46) as scheme S. Taking into consideration the statement of the test problems, in the algorithms it was assumed that $x \sim \bar{r}$, $y \sim \bar{z}$, $a = b = \alpha_0 = 0$, $\alpha_1 = \phi\alpha$ for Problem 1 and $\alpha_1 = -\pi/2$ for Problem 2. The integrals in L and C were approximated by the same order as the differential equations: the schemes A, B, *T-2*, *TM-2* used analogs of the midpoint and trapezoid rules, and schemes *T-4* and S – the Euler rule. So, e.g., in the case of a uniform grid the constants L and C at each iteration of algorithm *T-4* were calculated by the formulas

$$\begin{cases} L = \left\{ -2\pi\phi \left[h \sum\limits_{i=1}^{N-1} \bar{z}_i \bar{r}_i \cos\beta_i + \dfrac{h^2}{12} \left(\bar{z}_0 - \dfrac{1}{2}\phi \bar{r}_N \sin 2\alpha \right) \right] \right\}^{-1/3}, \\ C = \phi \left(\dfrac{2\sin\alpha}{\bar{r}_N} - \dfrac{1}{2}\mathrm{P} L^3 \bar{r}_N^2 \right) - \dfrac{\mathrm{Bo}}{\pi L \bar{r}_N^2}, \end{cases}$$

$$\begin{cases} L = \left[-2\pi h \left(\sum\limits_{i=1}^{N-1} \bar{r}_i^2 \sin\beta_i - \dfrac{1}{2}\bar{r}_N^2 \right) \right]^{-1/3}, \\ C = \dfrac{2}{\bar{r}_N^2} \left[-\bar{r}_N + \mathrm{W} L \left(h \sum\limits_{i=1}^{N-1} \bar{r}_i \cos^3\beta_i + \dfrac{h^2}{12} \right) \right] \end{cases}$$

where the first two formulas refer to Problem 1 and the other two – to Problem 2. The corresponding formulas for scheme *T-2* differ from the above by the absence of the terms containing h^2.

As a criterion for accuracy of an iterative solution, consideration was made of the discrepancy value of the difference equations. For example, iterations A and B continued unless the condition

$$\max_{k=1,2} \| \Lambda_k(\bar{r}^n, \bar{z}^n, F^n) \| \leqslant \varepsilon = 10^{-4}$$

was satisfied, and iterations T-2 and T-4 – unless the condition

$$\max_{0<i<N} \left| \frac{\beta_{i+1}^n - \beta_i^n}{h_{i+1}} - \Phi_{i+1}^n \right| \leqslant \varepsilon = 10^{-4}$$

was satisfied at any number $n = n(\varepsilon)$, where the operators Λ_k are of the form of (22).

Computations were made on uniform grids with steps $h = 1/100$ and $1/20$. Moreover, Problem 2 was solved on the adaptive grid with the number of partitions $N = 100$.

8.2. Results of tests

As the calculations have shown, because of the simplification of the recurrence procedures and the reduction of their number, in going from one iteration to another, both tangential schemes T-4, T-2, TM-2 and the spline-scheme S spent for one iteration a machine time smaller by a factor of 1.5–2 than the time spent by the schemes A and B.

8.2.1. Problem 1. Comparison with the known data of the stability theory has shown that a crisis of the computational process occurs at the same Bo_c and P_c as a collapse of equilibrium shapes. So, for an immovable pendent drop ($\mathrm{P} = 0$, $\phi = 1$) at $\alpha = 45°$ the theoretical value is $\mathrm{Bo}_c = 4.988$ and we have obtained numerically $\mathrm{Bo}_c = 4.982$ at $h = 1/100$ by using the scheme A; at $\alpha = 90°$ both theoretical and numerical values appeared to be equal to 2.265; and at $\alpha = 135°$ they turned out to be 0.579 and 0.580 respectively. It should be noted that the theoretical results presented were calculated by means of cubic-spline interpolation by the tabular data from [9, 10]. To avoid the influence of an interpolation error, the angle $\alpha = 1.523$ was considered in more detail. The exact value of $\mathrm{Bo}_c = 2.407$ for this angle is given in [9, 10]. As a result of the numerical experiment at $h = 1/20$, critical values of $\mathrm{Bo}_c = 2.3970 \pm \delta$ (schemes A and B), $2.4185 \pm \delta$ (scheme T-2), $2.4058 \pm \delta$ (scheme T-4) were obtained. At $h = 1/100$ all the schemes showed the same result $\mathrm{Bo}_c = 2.4058 \pm \delta$. The unremovable 0.001 difference between the analytical and numerical values of Bo_c can be caused by an error of the linear theory, which occurs due to the neglect of the second-order infinitesimal disturbances. We draw the attention to the high efficiency of the tangential scheme T-4 which provides the required accuracy δ not only at $h = 1/100$ but also on a rough grid at $h = 1/20$.

The equilibrium stability of a rotating drop has been studied theoretically only at $\mathrm{Bo} = 0$, $\alpha = 90°$. The critical value of the rotation parameter $\mathrm{P}_c = 4.7613 \pm \delta$ found numerically at $h = 1/100$ in fact does not differ from the theoretical one $\mathrm{P}_c = 4.763$ [9, 10].

An equally perfect agreement between theoretical and numerical values of the critical parameters was also observed in the problem on the magnetic-fluid seal stability [13, 19], for whose solution the scheme A was used, as well as in other problems. Thus, as a result of the numerical experiment, it has been found that all iterative algorithms presented adequately respond to a crisis of the equilibrium state of a free surface: if at some values of the problem parameters the equilibrium shapes collapse due to plane or axially symmetric disturbances, then a computational instability appears at the same critical values. Possibly, the point

is that the iterative process simulates a suitable unsteady-state process of development of perturbations.

8.2.2. Problem 2. Comparison of the algorithms by the most important convergence indices of the iterative process was made mainly in Problem 2. Table 1 contains the data on the convergence rate and computational stability as W grows. The left columns at each τ correspond to scheme A; the middle ones – to scheme B; and the right ones – to scheme T-4. The crosses stand for divergence of the iterative process; the sign ∞ marks situations, where the iterative process is of an oscillatory type with a bounded amplitude which does not damp at $n \to \infty$. The exhaustion of the W values was made at a step of 2.5. For each new variant, the solution obtained for the previous W served as an initial iterative approximation. The initial approximation for W = 2.5 is an exact solution at W = 0. As is seen, the scheme T-4 compares with the schemes A and B in the convergence rate but is much superior to them in stability.

Table 1. Indices of the convergence rate and stability of the iterative schemes on the uniform grid at $h = 1/100$ for Problem 2

W	Iteration number $n(\varepsilon)$											
	$\tau = 0.5$			$\tau = 0.1$			$\tau = 0.05$			$\tau = 0.01$		
2.5	19	30	42	113	14	239	231	30	484	1167	151	2449
5	210	×	38	123	29	219	249	21	444	1262	135	2246
7.5	×	—	41	129	∞	197	261	101	401	1320	114	2032
10	—	—	60	132	—	177	268	∞	363	1357	88	1847
12.5	—	—	141	134	—	159	273	—	330	1377	58	1694
15	—	—	∞	136	—	145	276	—	295	1391	∞	1550
...				...		...	...		...	...		...
27.5	—	—	—	209	—	170	274	—	260	1381	—	1143
30	—	—	—	417	—	191	272	—	265	1370	—	1188
32.5	—	—	—	×	—	216	270	—	249	1357	—	1127
...						...	...		...	...		...
40	—	—	—	—	—	496	268	—	256	1313	—	1127
42.5	—	—	—	—	—	992	386	—	257	1301	—	1086
45	—	—	—	—	—	∞	833	—	261	1292	—	1044
47.5	—	—	—	—	—	—	×	—	263	1295	—	1068
...									...	...		...
55	—	—	—	—	—	—	—	—	307	2260	—	1039
57.5	—	—	—	—	—	—	—	—	332	3424	—	1094
60	—	—	—	—	—	—	—	—	374	∞	—	1132
...									...			...
77.5	—	—	—	—	—	—	—	—	1691	—	—	1145
80	—	—	—	—	—	—	—	—	4438	—	—	1125
82.5	—	—	—	—	—	—	—	—	∞	—	—	1141
...												...
145	—	—	—	—	—	—	—	—	—	—	—	3933
147.5	—	—	—	—	—	—	—	—	—	—	—	4725
150	—	—	—	—	—	—	—	—	—	—	—	>5000

Let us emphasize the inconsistency of the scheme B in the case of strongly curved (locally disturbed) surfaces characteristic of magnetizing and electrically conducting fluids in high fields. Indeed, the stability domain of the scheme B is limited by the value $\mathrm{W} \approx 15$ at which the curvature $K(0)$ only 5.5 times exceeds the curvature, K_0, of the spherical drop at $\mathrm{W} = 0$. For comparison: at $\mathrm{W} = 150$ limiting for the scheme *T-4* at $h = 1/100$ the relative curvature attains $K(0)/K_0 = 47.6$.

At the same time, when capillary surfaces are calculated in a gravitational field, the scheme B can be fairly efficient [11]. In this case, the maximum value of the curvature K, as a rule, does not differ considerably from the spherical surface curvature realized under zero-gravity, and the physical instability occurs earlier than the computational one. So, in Problem 1 at $\mathrm{P} = 0$, $\phi = 1$, $\alpha = 1.523$ the equilibrium crisis that occurred at $\mathrm{Bo} = \mathrm{Bo}_c$ is defined by the critical curvature $K(0)/K_0 = 1.61$, which in Problem 2 corresponds to the value of $\mathrm{W} = 2.5$ belonging to the stability domains of all the schemes.

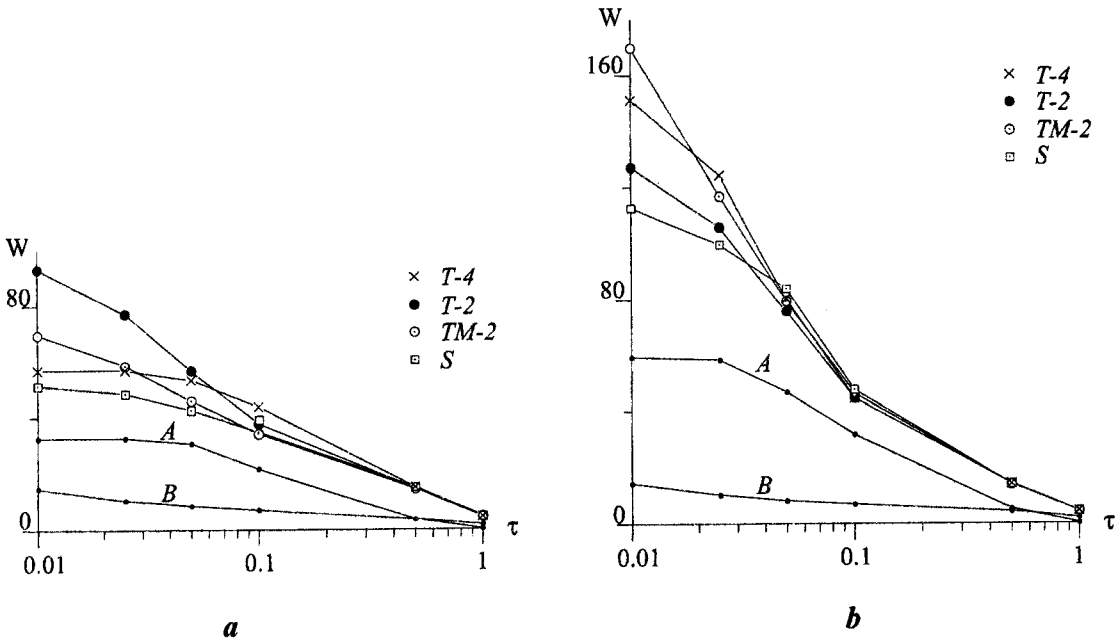

Figure 1. Boundaries of computational stability of the iterative schemes on the uniform grids at $h = 1/20$ (a) and $h = 1/100$ (b). Problem 2

Fig. 1 plots the computational stability boundaries of the iterative schemes. Each curve divides the domain (W, τ) into two subdomains: the computational stability domain lies below the curve while the computational instability domain lies above it. Note that the stability domain of the scheme B does not depend on the step h, and the stability of the remaining schemes is considerably improved as h decreases. It is seen that at both $h = 1/20$ and $h = 1/100$ the tangential schemes *T-4*, *T-2*, and *TM-2* as well as the spline-scheme S are stable over a much wider range of values of the magnetic parameter W than the iteration-difference schemes A and B. And this advantage becomes more and more perceptible as the grid is refined. The fact that the scheme *T-2* has shown better stabilizing properties on the rough grid than the scheme *T-4* of the same type can be explained by the higher order of approximation of the latter, because an increase in the order of approximation usually leads to more severe restrictions on the grid step in stability conditions. Also, let us note good stabilizing properties of the scheme *TM-2* shown on the two grids. The spline-

scheme S compares somewhat unfavorably with the tangential schemes in stability. Possibly, the reason is that the test problem is classified with moving boundary problems, and the tangential method is most adapted to them.

8.2.3. Adaptive grid. The adaptive grid has proved to be a powerful tool for stabilizing iterations as the surface curvature grows. If on a uniform grid with a step $h = 1/100$ the stability domain of the scheme *T-4* is limited by the value of $W \approx 150$ (see Table 1), then on the adaptive grid the stability boundary moves to $W = 4800$. Because of the optimal distribution of the nodes s_i, a high accuracy of results is provided, allowing the peak-shaped apex formation to be described as W grows (Fig. 2). A close-up view of such an apex is shown in Fig. 2,e. Its curvature 1491 times exceeds that of the spherical drop at $W = 0$. It is interesting that more than half of the nodes s_i are concentrated on the depicted fragment of the surface meridian, although its length is less than 1/400 of the total meridian length. As the apex is approached, the monotonic increase in the curvature is accompanied by a decreasing in the steps $h_i = \bar{s}_i - \bar{s}_{i-1}$. So, at $W = 4800$ the minimal step attains a value of $h_1 = 8 \cdot 10^{-7}$ and the maximal one – $h_N = 0.06$.

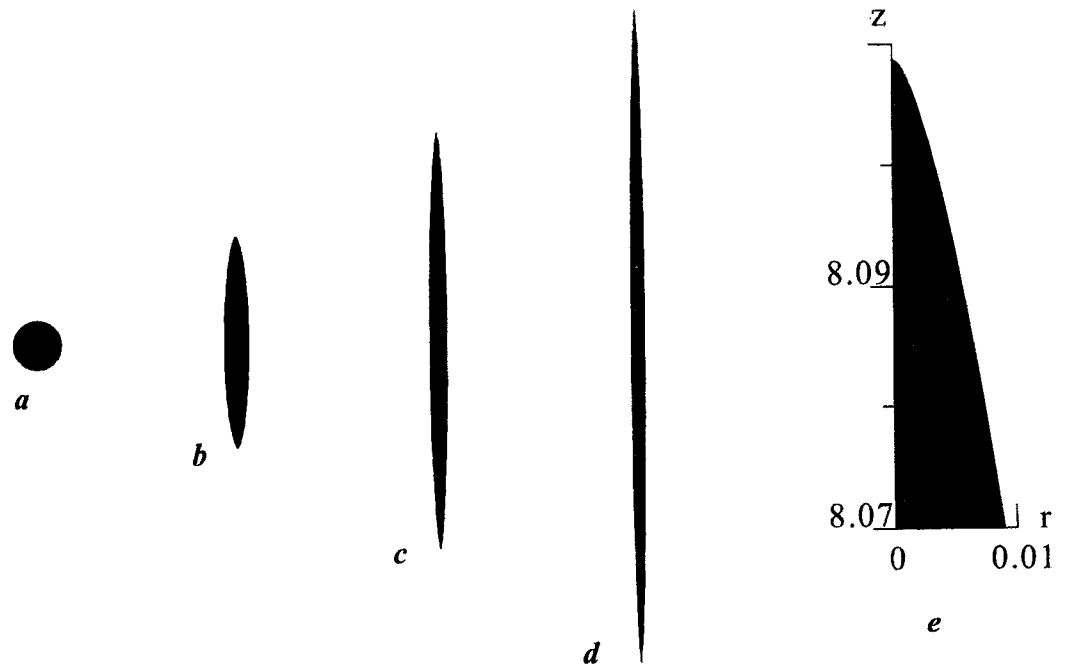

Figure 2. Drop deformation with increasing magnetic parameter W: *a*, $W = 0$; *b*, 100; *c*, 1000; *d*, 4800; *e*, peak-shaped apex of the drop at $W = 4800$. Problem 2

For the scheme A, the limiting values of the magnetic parameter have proved to be much lower: $W \approx 60$ (uniform grid) and $W \approx 150$ (adaptive grid). However, the stabilizing properties of the scheme A are considerably improved by means of the coordinate-wise relaxation procedure described below: due to it a solution was obtained within $W \leqslant 750$. However, in the case of the scheme *T-4*, this procedure did not yield a positive result.

8.2.4. Coordinate-wise relaxation. On the basis of the known theoretical results concerning the overrelaxation method, it is reasonable to assume that the optimal values of τ in

the above iterative algorithms depend on the grid step. Namely, the optimal value increases in the range of admissible values $0 < \tau < \tau^* \leqslant 2$ as the grid is refined. In solving equilibrium capillary-surface problems on nonuniform grids, the dependence of the parameter $\tau = \tau_i$ on the step h_i can be assigned in the approximate form

$$\tau = \tau_i = \bar{\tau}\left(1 - \frac{h_i - h}{A + B(h_i - h)}\right), \quad i = 1, 2, \ldots, N;$$

$$A = \frac{\tau^* h(1-h)}{\tau^* - \bar{\tau}}, \quad B = \frac{\tau^*(1-h) \dot{-} \bar{\tau}}{\tau^* - \bar{\tau}}$$

where τ^* and $\bar{\tau}$ are coefficients evaluated from the numerical experiment, $\bar{\tau}$ is some average value in the range of admissible values which is appropriate to the average step $h_i = h = 1/N$. Notice that the maximum $\tau_i = \tau^*$ and the minimum $\tau_i = 0$ of the relaxation parameter are attained only in the limiting cases $h_i = 0$ and $h_i = 1$.

References

[1] D. Anderson, J. Tannehill, and R. Pletcher, *Computational Fluid Dynamics and Heat Transfer*, Hemisphere Publ. Corp., New York, 1984.

[2] V. G. Bashtovoi, A. M. Budnik, V. K. Polevikov, and A. G. Reks, *Doubly connected equilibrium configurations of ferrofluid in magnetic field of vertical conductor*, Magnetohydrodynamics, **20** (1984), No. 2, pp. 144–150; translation from Magn. Gidrodin., 1984, No. 2, pp. 47–53.

[3] B. M. Berkovsky and V. K. Polevikov, *Numerical simulation of instability in singly connected axisymmetrical forms of a magnetic liquid*, Magnetohydrodynamics, **19** (1983), No. 4, pp. 396–402; translation from Magn. Gidrodin., 1983, No. 4, pp. 60–66.

[4] B. M. Berkovsky, V. F. Medvedev, and M. S. Krakov, *Magnetic Fluids: Engineering Applications*, Oxford University Press, 1993.

[5] A. M. Budnik and V. K. Polevikov, *Axially symmetric equilibrium shapes of a fluid in a toroidal vessel under zero-gravity*, Izv. Akad. Nauk SSSR, Mekh. Zhidk. Gaza, 1986, No. 6, pp. 154–156.

[6] A. M. Budnik and V. K. Polevikov, *Numerical study of equilibrium forms of magnetic fluid including magnetic field disturbances*, J. Magn. Magn. Mater., **65** (1987), No. 2-3, pp. 335–338.

[7] R. Finn, *Equilibrium Capillary Surfaces*, Springer-Verlag, New York, 1986.

[8] *Magnetic Fluids and Applications Handbook*, Eds B. Berkovski and V. Bashtovoi, Begel House Inc. Publ., New York, 1996.

[9] A. D. Myshkis, V. G. Babskii, N. D. Kopachevskii, L. A. Slobozhanin, and A. D. Tyuptsov, *Low-Gravity Fluid Mechanics. Mathematical Theory of Capillary Phenomena*, Springer-Verlag, Berlin, 1987.

[10] A. D. Myshkis, V. G. Babskii, M. Yu. Zhukov, N. D. Kopachevskii, L. A. Slobozhanin, and A. D. Tyuptsov, *Methods of Solving Hydrodynamic Problems for Low-Gravity Conditions*, Naukova Dumka, Kiev, 1992.

[11] V. K. Polevikov and V. M. Denisenko, *Numerical study of equilibrium shapes of a drop rotating in gravitational field*, Vestn. Beloruss. Gos. Univ., Ser1, Fiz. Mat. Mech., 1985, No. 2, pp. 37–41, In Russian.

[12] V. K. Polevikov, *Application of adaptive grids to calculate the free surface in problems on statics of a magnetic fluid*, Differ. Equations, **30** (1994), No. 12, pp. 1973–1978; translation from Differ. Uravn., **30** (1994), No. 12, pp. 2146-2152.

[13] V. K. Polevikov, *Stability of a static magnetic-fluid seal under the action of an external pressure drop*, Fluid Dyn., **32** (1997), No. 3, pp. 457–461; translation from Izv. Akad. Nauk, Mekh. Zidk. Gaza, 1997, No. 3, pp. 170–175.

[14] V. K. Polevikov, *Numerical Modeling of Equilibrium Capillary Surfaces: Some Methods and Results*, Preprint 10-98, Otto-von-Guericke University of Magdeburg, Faculty of Mathematics, Magdeburg, 1998.

[15] V. K. Polevikov, *Methods for numerical modeling of equilibrium capillary surfaces*, Differ. Equations, **35** (1999), No. 7, pp. 985–991; translation from Differ. Uravn., **35** (1999), No. 7, pp. 975–981.

[16] R. E. Rosensweig, *Ferrohydrodynamics*, Dover Publ. Inc., New York, 1997.

[17] A. A. Samarskii and E. S. Nikolaev, *Numerical Methods for Grid Equations, Volume 1: Direct Methods*, Birkhaüser Verlag, Basel, 1989.

[18] A. N. Vislovich and V. K. Polevikov, *Effect of the centrifugal and capillary forces on the free surface shape of a magnetic liquid seal*, Magnetohydrodynamics, **30** (1994), No. 1, pp. 67–74; translation from Magn. Gidrodin. 1994, No. 1, pp. 77–86.

[19] A. N. Vislovich and V. K. Polevikov, *Concerning numerical simulation of the failure of a magnetic-fluid seal with a rotary outer profiled cylinder*, J. Eng. Phys. Thermophys., **70** (1997), No. 1, pp. 107–112; translation from Inzh.-Fiz. Zh., **70** (1997), No. 1, pp. 105–110.

Received 25 Jun. 2003
Revised 4 Feb. 2004